Master Thesis in Geographical Information Science nr 75

Sensitivity Analysis and Calibration of Multi Energy Balance Land Surface Model Parameters

Author: Kim Friberg

2017
Department of
Physical Geography and Ecosystem Science
Centre for Geographical Information Systems
Lund University
Sölvegatan 12
S-223 62 Lund
Sweden

Friberg, K (2017). Sensitivity Analysis and Calibration of Multi Energy Balance Land Surface Model Parameters.
Master degree thesis, 30 credits in Geographical Information Systems (GIS) Department of Physical Geography and Ecosystem Science, Lund University

Sensitivity Analysis and Calibration of Multi Energy Balance Land Surface Model Parameters

Kim Friberg
Master degree thesis, 30 credits, in Master in Geographical Information Science
Department of Physical Geography and Ecosystem Science, Lund University

Supervisors
Patrick Samuelsson
Researcher at the Swedish Hydrological and Meteorological Institute (SMHI)

Anna Maria Jönsson
Professor at the Department of Physical Geography and Ecosystem Science, Lund University

Abstract

Flows of energy between the atmosphere, the oceans and the land surfaces drive weather and climate on Earth. Increased understanding of these processes is crucial to successfully predict and address the challenges of climate change. Land surface models (LSM) are mathematical models designed to mimic natural processes and evolution of land surfaces with the basic task to simulate surface-atmosphere energy flows. Within the SURFace EXternalisée modeling platform (SURFEX), developed by Météo-France and a suite of international partners, a new LSM called the Interaction Soil Biosphere Atmosphere model - Multi Energy Balance (ISBA-MEB) has been developed. There are however still uncertainties in how to accurately prescribe model parameters used to numerically define the physiography and natural processes of modelled land surfaces which consequently results in uncertainties in modelled outputs. In the present study, Quasi-Monte Carlo simulations based on Sobol sensitivity analysis was applied to explore the uncertainty contribution of individual parameters to modelled surface-atmosphere turbulent sensible and latent heat fluxes in forest environments. Those parameters to which modelled fluxes were identified as significantly sensitive were then calibrated by generating multiple sets of parameter values with the Latin Hypercube sampling technique on which the model was run to identify what parameter values generated the least amount of model output bias and to evaluate how much model output uncertainty could be reduced. To explore variations in parameter sensitivity and optimal parameter prescriptions between forest environments, four separate forest areas with varying vegetation types and climate classifications were modelled. Results disclose that the level of uncertainty contribution of individual parameters varies between forest environments. Three parameters were however identified to contribute with significantly output uncertainty; 1) the ration between roughness length of momentum and thermal roughness length, 2) the heat capacity of vegetation and soil and 3) the leaf orientation at canopy bottom. Calibrating these parameters marginally reduced model output uncertainty at all study areas.

Keywords: Physical Geography, Land Surface Model, Multi Energy Balance, Sensitivity Analysis, Sobol’s Method, Parameter Calibration, FLUXNET.

Acknowledgement

I would like to start off by expressing my deepest gratitude to my supervisors - thank you Patrick Samuelsson at SMHI and Anna Maria Jönsson at Lund University for guiding, inspiring and challenging me throughout the course of this project. Furthermore, I wish to thank the SURFEX development team and the researchers at SMHI for including me in the community. Finally, I´d like to thank my family for supporting and motivating me during my studies.

Table of Contents

List of Abbreviations

LSM – Land Surface Model
SURFEX – SURFace EXternalisée (modelling platform)
ISBA – Interaction Soil Biosphere Atmosphere model
MEB – Multi Energy Balance
SMHI – Swedish Hydrological and Meteorological Institute
Rn – Net Radiation
LE – Latent Heat
H – Sensible Heat
Gflux – Ground Heat Flux

List of Figures

List of Tables

List of Equations

1 Introduction

In principle, all the energy available on Earth originates from the sun intercepted as short wave electromagnetic radiation. A proportion of the energy is instantly reflected back to space while remaining quantities is absorbed by the planet and circulates the atmosphere, oceans and land surfaces before ultimately being emitted back to space (Barry & Chorley, 2010). These energy flows drive the weather and climate phenomena on Earth. Increased understanding of these drivers has been recognized by the scientific community as crucial to successfully predict and address the challenges of climate change (Petropoulos et al., 2014).

As one of the fundamental components of this system, the land surface exchange energy with the atmosphere and the ground (Barry & Chorley, 2010). As insolation heat terrestrial surfaces a surplus in the land surface energy budget is generated. To attain energy balance, the surplus is transported via turbulence to the atmosphere as heat (i.e. sensible heat) and moisture (i.e. latent heat) and via heat conduction into the ground. In contrast, absence of insolation causes a surface energy deficit which instead is compensated by absorbing energy from the surroundings. In forest areas the canopy significantly alters patterns of incoming and outgoing land surface energy flows by absorbing and reflecting a proportion of incoming energy as well as trapping energy already in the forest. These factors is in turn governed by, and vary with, forest site specific properties such as age, height and density of trees as well as vegetation specific properties such as the shape, size and density of canopy leafs (Liming et al., 2012). In the presence of a forest floor snowpack conditions for incoming energy is further altered as the surface albedo, and thus reflected energy quantities, is increased as well as for outgoing energy as snow insulates the surface (Decharme et al., 2016).

Land surface models (LSM) are mathematical models designed to mimic the natural processes and evolution of terrestrial surfaces with the basic task to simulate the energy flows of the land surface energy budget (Zhao & Li, 2015). Météo-France and a suite of international partners have developed a LSM called the Interaction Soil Biosphere Atmosphere model - Multi Energy Balance (ISBA-MEB) (Boone et al., 2017). In contrast to its predecessor (ISBA), which is a single energy balance LSM that treat all components of the (snow free) land surface as a composite energy budget, ISBA-MEB enables separation of landscape components such as the land surface, canopy and snowpack into distinct energy budgets for a more realistic land surface representation. Napoly et al. (2016) showed that ISBA-MEB in general enable more realistic land surface energy budget simulations in forest areas than ISBA. However, there are still uncertainties in how to prescribe the numerical parameters that are used to provide the LSM with information on the characteristics of modelled landscapes.

Uncertainties in how to prescribe parameters consequently lead to uncertainties in modeled outputs. A common approach in addressing this issue is to identify parameters to which the models ability to accurately simulate its outputs is highly sensitive and to adjust the prescriptions of these until simulations better correlate with reality (Muleta & Nicklow, 2005). Furthermore, as the landscape characteristics influencing the land surface energy flows vary between forests, so do the influence of parameters on the models ability to accurately simulate its outputs. Consequently, parameter sensitivity often varies between forests and thus optimal results are achieved by site specific parameter calibration (Hou et al., 2015).

1.1 Objective

The aim of the present study is to explore how sensitive ISBA-MEB simulated latent and sensible turbulent heat fluxes are to a selected set of uncertain parameters, to explore if parameter sensitivity patterns vary between forest environments and to evaluate how much model output improvement can be achieved by identifying site specific optimal numerical prescription for parameters identified as the top most sensitive. To achieve this, the experimental setting is to be multiple forest areas with seasonal snow coverage of different climate classifications and vegetation types. The study will be guided by the following research questions:

- To which of the tested parameters are modelled sensible and latent heat flux most sensitive in different forest environments?
- How do the values of the calibrated parameters vary between forest environments?
- How much improvement in modelled sensible and latent heat fluxes can be achieved by calibrating highly sensitive parameters in different forest environments?

2 Background

Meteorology is the science of weather and climate phenomena occurring within the atmosphere at different space and timescales; from gusts of winds that swirl up some leaves for a few seconds to the large scale wind systems of the global climate system (Barry & Chorley, 2010). The particular focus of this study is on micro-meteorology within the planetary boundary layer where the lower boundary atmosphere meets and interacts with the surface of the planet. This background section is dispositioned into a first part in which the concept of the energy budget of terrestrial surfaces is presented, a second part in which the concepts and components of LSM are presented and finally a third part in which parameter sensitivity analysis and parameter calibration is discussed.

2.1 The land surface energy budget

Principally all energy available on Earth has been intercepted as short wave (SW) electromagnetic radiation from the sun and is either instantly reflected back to space by clouds, atmospheric particles and the planet's surface or absorbed by, and circulates, the atmosphere, the oceans and the land surface (Barry & Chorley, 2010). To attain energy balance in the planetary energy budget, energy quantities equal to those absorbed must ultimately be emitted back to space resulting in a constant flow on incoming and outgoing energy (Wild et al., 2014). It is these flows of energy that drive the planetary weather and climate phenomena.

Much like Earth constantly exchange energy with space, so does the land surface with the atmosphere and the ground to attain balance in the land surface energy budget (Barry & Chorley, 2010). During day time the land surface is supplied with SW radiation from the sun and long wave (LW) radiation from the atmosphere which is offset by day time and night time emissions of thermal LW radiation i.e. thermal cooling. The net of these radiation quantities constitute the surface net radiation (Rn). Day time energy contributions normally surpass those of the thermal cooling emissions resulting in a surface Rn surplus. During night time, in the absence of insolation, thermal cooling emissions instead generate Rn energy deficit. The equation for the surface energy budget is often written as:

$$Rn = G + H + LE \tag{1}$$

where G, H and LE denote ground heat flux, sensible heat flux and latent heat flux, respectively. H can be described as heat that can be sensed, thus *sensible* heat. When an entity absorbs or emits H, the temperature of that entity changes e.g. oceans absorbing insolation experience increased water temperature. LE is energy released from, or absorbed by, a substance during a phase change e.g. energy leaving boiling water as vapour. LE is mainly associated with evapotranspiration and is sometimes expresses as an equivalent to that energy transport medium. The final component of the energy balance equation is G which denotes heat transferred by the mode of conduction in soils. A generalized description of day time and night time energy flows is given in Figure 1.

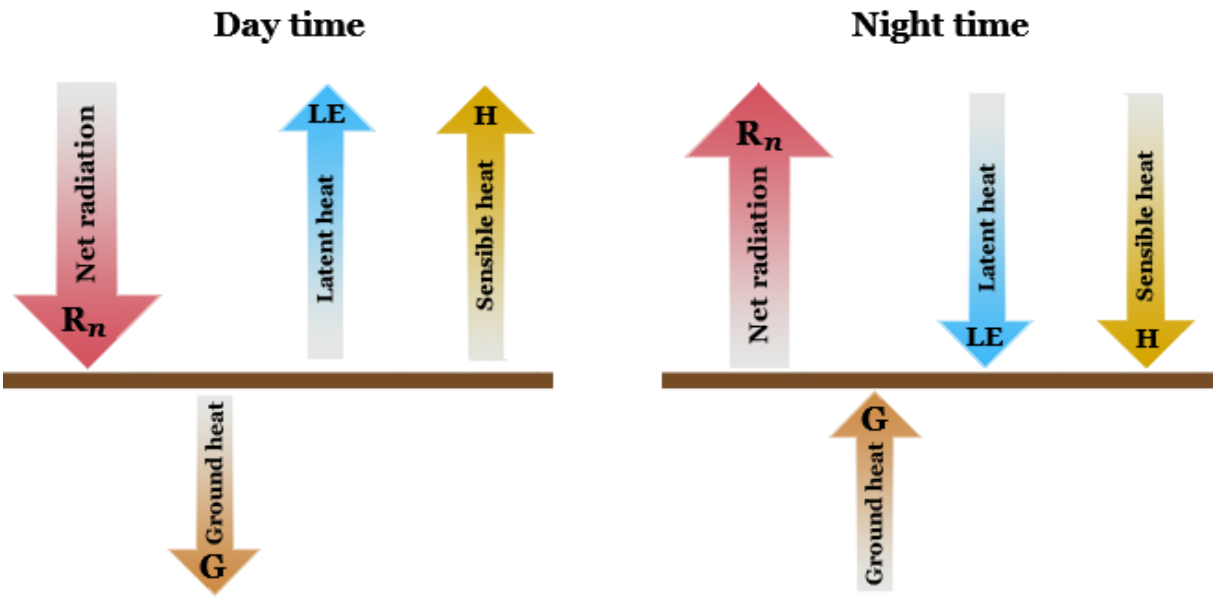

Figure 1. *Simplified sketch of day- and night-time energy flows of the land surface energy budget. Vertical brown lines represent a simple land surface. Day time surplus surface net radiation (Rn) is partitioned into latent (LE) and sensible (H) turbulent heat fluxes to the atmosphere and diffusion of heat (G) into the ground. In contrast, night time surface Rn deficit is compensated by contributions of heat fluxes from the atmosphere and the ground.*

2.1.1 Turbulent flux

Turbulence is generated by hot air rising from the oceans and land surfaces of Earth. Within the planetary boundary layer, LE and H is transported by mechanical and convective diffusion processes i.e. turbulent and eddy diffusion (Barry & Chorley, 2010). Turbulent diffusion is still an unresolved apparently random and chaotic phenomenon instantaneously transporting momentum, water and heat at a timescale of a second or less. The concept of atmospheric eddy diffusion is however better understood in which a wind is described as a horizontal flow of rotating eddys that transport parcel of air (Figure 2). Each parcel store momentum, water and heat which is transported either between the land surface and the atmosphere, or between different horizontal atmospheric layers. The size of eddies range from a few cm to about two meters in diameter above a heated surface and grade into dust devils and tornados at greater meteorological scales. The term turbulent flux denotes the net transportation of a specific entity crossing a delimited area at a specific time unit. Turbulent fluxes constitute the majority of the heat transports of the land surface energy budget. A key aspect affecting the characteristics of winds is surface roughness (Pelletier & Field, 2016). A wind blowing over a smoot surface is less exposed to friction than a wind blowing over a rougher surface with more obstacles like scattered trees or an uneven landscape. When winds collide with obstacles of rough surfaces turbulence is onset.

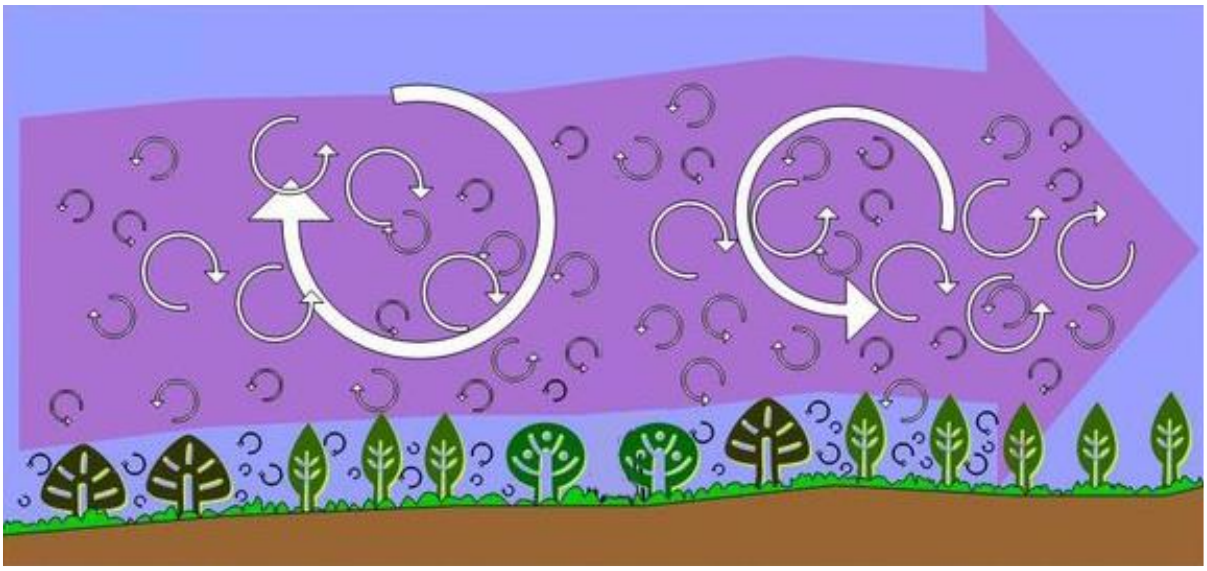

Figure 2. *Conceptual sketch of eddy diffusion. A wind (purple arrow) blowing over a forest consist of rotating eddies (white arrows) of different sizes that transport momentum, heat and moisture between the land surface and the atmosphere as well as between different levels within the atmosphere (modified figure from Burba & Anderson, 2010).*

2.1.2 Ground heat flux

The principal energy transport mode in soils is conduction and the conduction capacity of a soil is a function of the solid fraction (i.e. particle size, mineral type and organic content) and the density and water content (Sauer & Horton, 2005). Besides differences in these properties between soil types, they often vary spatially within the same soil type, between soil layers as well as over time. Consequently, the magnitude of G may vary greatly between different types of soils and land covers.

2.1.3 Energy budget in forest areas

Forest canopies significantly alter patterns of incoming and outgoing radiation to the land surface (Barry & Chorley, 2010). The quantities of SW and LW that reach the forest floor by penetrating the canopy (i.e. forest crown and forest trunk) is governed by a range of site specific factors such as the density, distribution, height and age of the trees as well as vegetation specific factors such as dispersion, angular orientation and areal coverage of leafs and branches (Liming et al., 2012). Many of these factors also vary over the year which in combination with weather variations alters the patterns of incoming and outgoing radiation (Carrer et al., 2013). Radiation that does not penetrate the canopy is instead either reflected, proportional to the specific albedo of the vegetation species, or absorbed by the vegetation. In addition, a forest canopy also acts as an insulation trapping the energy already in the forest environment. Consequently, energy fluxes of forest land surface energy budgets vary with site specific ecosystem characteristics such as forest and vegetation properties.

2.1.4 Energy budget in the presence of a snowpack

The presence of a snowpack significantly alters conditions and patterns of land surface energy interception and flux partitioning (Decharme et al., 2016). Even though the albedo of snow varies with factors like density, temperature and age, it is in general always greater than the albedo of the surface it covers. Thus, a snowpack decreasing energy quantities absorbed by

the surface as the reflectance of incoming energy is increased. In addition, a snowpack insulates the surface inhibiting energy loss to the atmosphere.

2.2 Land Surface Models

LSM are mathematical models that, based on theories and hypothesis, are designed to mimic ecosystem functions and processes with the basic task to simulate the partitioning of land surface Rn into emissions of LW thermal radiation, turbulent LE and H heat fluxes to the atmosphere and G heat diffusion in the ground (Zhao & Li, 2015). In addition, LSM provide information on the state and evolution of the land surface, weather and climate. Therefore LSM has become an import tools in weather forecasting, hydrological and climate models.

The core of a LSM is the model structure consisting of algorithms mimicking ecosystem functions and natural processes of the modelled environment. The modeling structure is composed of several sub-models each designed to mimic specific biological, geological, and chemical process of land surface component such as soil, snow and vegetation (Overgaard et al., 2006). The modelling structure do however not have any inherit knowledge of the characteristics of modelled environments and therefore such information need to be provided. Atmospheric forcing data such as intercepted radiation quantities, precipitation, air pressure and wind speed is provided either be directly by the modeller (i.e. offline mode) or by coupling the LSM to an atmospheric model (i.e. coupled mode) (Zhao & Li, 2015). Information on the surface characteristics of a modelled environment is provided by the use of numerical parameters. Most parameters of current generation LSM have physical meaning which means that their numerical value is a direct translation of the natural state of what they represent and these can therefore be prescribed to measured values. Model parameters can further be divided into two main groups; physiography parameters and process parameters (Masson et al., 2013). As the name suggests, physiography parameters are applied to provide the model with the information on the physiography of a landscape e.g. topography, soil type and vegetation characteristics. Process parameters are factors involved in the computation of the natural processes and evolution of land surfaces. Parameters are either prescribed according to measurements by the modeller or by coupling the model to databases. In general terms, the model structure, atmospheric forcing data, the parameters and simulated output data are the four main components of any LSM (Figure 3).

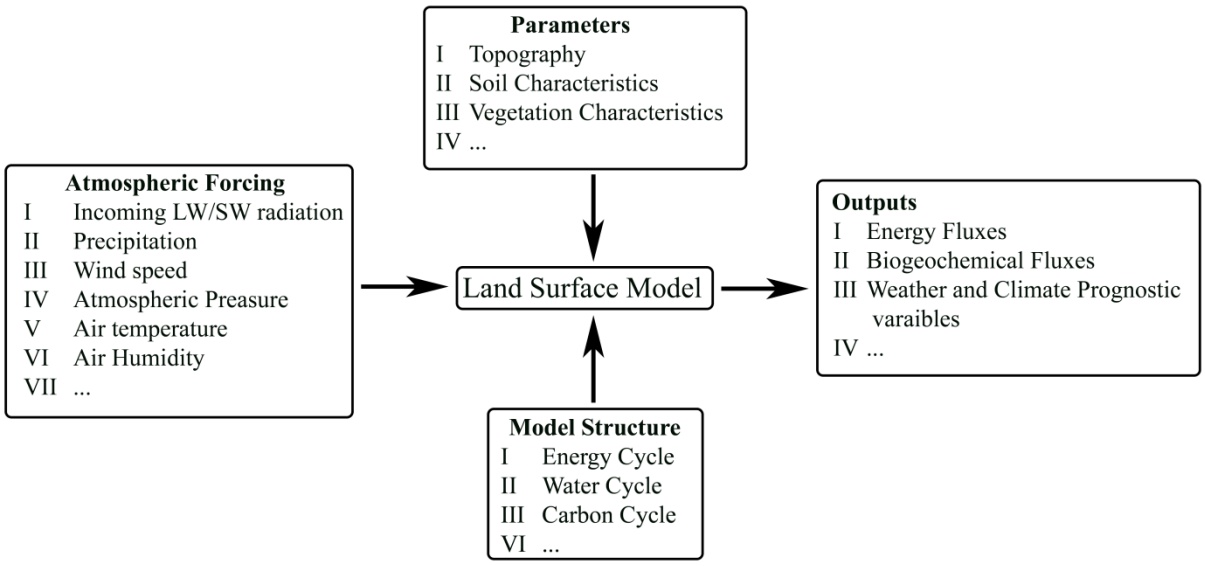

Figure 3. *The four main components of LSM. Atmospheric forcing data is processed by the model structure in the context of the landscape characteristics defined by the parameters to generate model outputs (modified figure from Zhao & Li, 2015).*

2.2.1 SURFEX

SURFace EXternalisée platform (SURFEX) is a modelling platform developed by the French national meteorological service Météo-France and a suite of international partners (Masson et al., 2013) including the Swedish Hydrological and Meteorological Institute (SMHI). It is designed to simulate surface-atmosphere fluxes and evolution of four types of surfaces: town, nature, inland water and ocean. SURFEX enable flux simulation of momentum, heat and water as well as carbon dioxide, chemical species, continental aerosols, sea salt and snow particles. It can be run in offline mode or coupled to hydrological or atmospheric models and is used in hydrology, numerical weather prediction and climate simulations. Parameters can be prescribed either by the modeller of by couplings to databases.

2.2.2 ISBA-MEB

Within the SURFEX framework the operational LSM for modeling landscape evolution and surface-atmosphere interactions is the Interaction Soil Biosphere Atmosphere model (ISBA) (Masson et al., 2013). By design all components of the surface landscape such as soil, vegetation and snow is treated as a single composite energy budget. This modeling approach has reached its limits and to remain consistent with the LSM development and to respond to current and future demands a new Multi Energy Balance (MEB) LSM has been developed (Boone et al., 2017). In contrast to the operational ISBA, this new modelling scheme called ISBA-MEB enables separation of surface components into three layers with distinct energy budgets. With this approach the separate functions of the landscape components as well as the energy exchanges between these, the ground and the atmosphere can be better represented which in turn facilitates better modelling of the surface energy balance. In Figure 4 a schematic diagram illustrate how turbulent energy flows is simulated amongst the land surface components and the atmosphere in ISBA-MEB; ground is coloured brown, canopy green and snow turquoise. There are six energy flow pathways between expressed as aerodynamic resistances (R_a): (1) the canopy not covered by snow and the canopy air, R_{avg-c},

(2) the ground surface not covered by snow and the canopy air, R_{ag-c}, (3) the forest floor snow surface and the canopy air, R_{an-c}, (4) the canopy part covered by forest floor based snow and the canopy air, R_{avn-c}, (5) the canopy air and the atmosphere, R_{ac-a} ,and (6) the direct interaction between the forest floor based snow surface and the atmosphere, R_{an-a}. It can also be seen in this picture that the snowpack and ground can be further divided into several layers for better representation of characteristics at different depths.

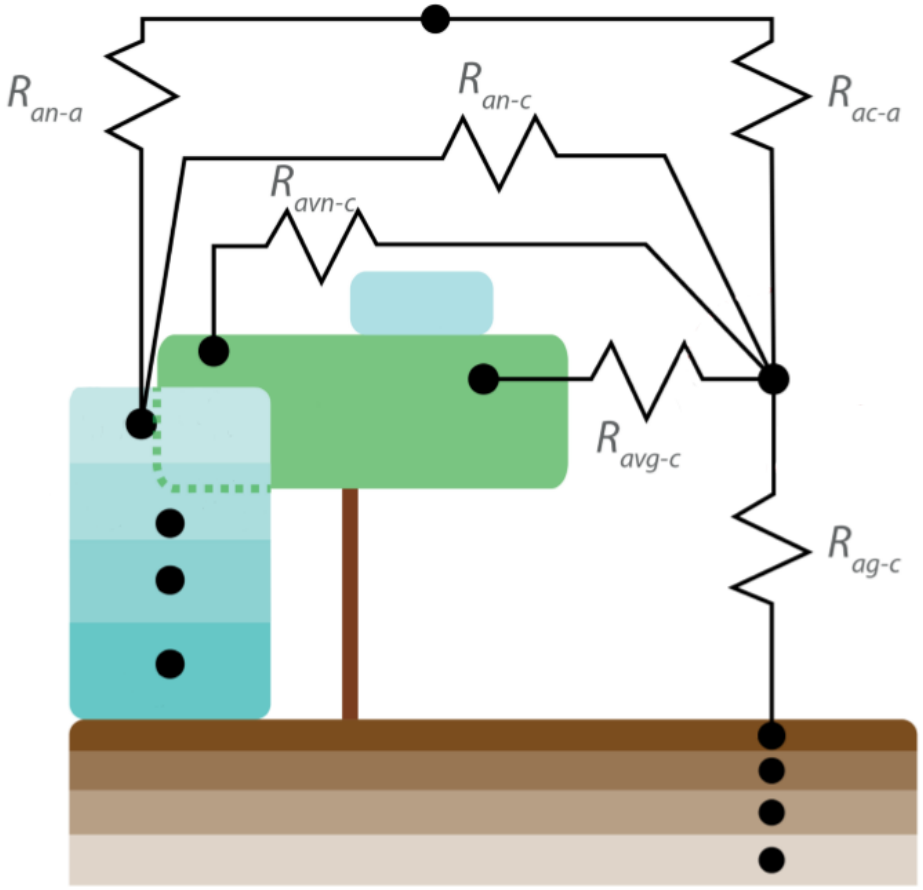

Figure 4. *The six pathways for turbulent fluxes in terrestrial surfaces between soils (brown), snow (tortoise), canopy (green) and the atmosphere (modified figure from Boone et al., 2017).*

At this point in time Napoly et.al (2016) offers the only previously published study in which the performance of ISBA-MEB is tested and the results show that ISBA-MEB enables more accurate simulations of Rn partitioning into LE, H and G fluxes than the ISBA LSM.

2.3 Parameter calibration

LSM, like all other models, are per definition simplified representations of reality and simulated outputs are only as realistic as the assumptions, hypothesis and theories on which the model structure is built and the quality of the input data. In the process of model development an imperative step is to identify model components whose definitions is uncertain, and consequently impact the reliability of simulated outputs and to adjust these components until outputs closely match observed behaviours of the target environment – this is what is commonly referred to as calibration (Muleta & Nicklow, 2005). For LSM there are four sources of such uncertainty; uncertainties in the input data such as atmospheric forcing data, uncertainties in output data used for calibration, model structure uncertainties such as

neglect of important land surface processes or misrepresentation of included processes, and finally parameter uncertainties (Hou et al., 2015). The focus of this study is on the later and more precisely on process parameters.

The term parameter sensitivity explains the level of influence a parameter has on a models ability to accurately compute its output in a given modelling environment (Saltelli, 2008). Consequently, misrepresentative prescriptions of sensitive parameter generate more uncertainty and potentially more bias in modelled outputs than does less sensitive parameters. In addition, as current generation LSM are highly non-linear mathematical models and process parameters are factors in the model algorithms, the numerical prescription of one parameter often influence the behaviours of other parameters which in turn further generate output bias if a parameter prescription is misrepresentative. Parameter sensitivity is therefore often expressed as the first order sensitivity due to a parameters direct effect as well as parameters higher order sensitivity due to interactions.

It is often argued that one of the most appealing aspects of modern LSM is that the parameters are physically based. However, it is hard to exactly prescribe these since the aspects they represent and the natural processes in which they are involved are highly spatially heterogeneous and differ between environments, climate classifications and vegetation species. For optimal simulation results, such environmental variations need to be accounted for by adjusting parameter prescriptions according to the specific characteristics of simulated environments (Chaney et al., 2016). In addition, differences in ecosystem characteristics between forest sites also affect to what extent a model is sensitive to specific parameters (Hou et al., 2015). As such, parameter sensitivity patterns often vary between forest environments.

Raoult et.al (2016) argues that for objective, reproducible and optimal results calibration of parameters included in complex non-linear mathematical models must be conducted by applying established statistical methodologies. A commonly applied such methodology include two main steps. First, a sensitivity analysis is conducted to discern to which parameters one or more model output variables are sensitive. Second, that or those parameters identified as to be associated with the highest level of sensitivity become subjects of the calibration process itself while less sensitive parameters are set to default values.

2.3.1 Sensitivity analysis

The concept of sensitivity analysis has been described by Saltelli (2008) as the study of how uncertainty in model outputs can be apportioned to different sources of uncertainty in model inputs. Sensitivity analysis methods are separated into local and global methods. In local methods the first order uncertainty contribution of parameters is estimated whereas the global methods are applied to estimate the higher order uncertainty contribution in addition to the first order. Pianosi et al. (2017) argues that analysing parameter sensitivity of LSM with complex non-linear model structure and numerous complex parameter interactions demands the use of global approaches. For instance, Hou et al. (2015) applied both local and global sensitivity analyses on LSM parameters which generated similar sensitivity patterns among the global analysis, but these results differed in comparison to the results of the local methods. The drawn conclusion was that the local method was unable to generate valid results due to

the complexity of model parameter interactions. Chaney et al. (2016) also emphasised the need for global analysis as a single parameter can influence as many as 20 other parameter of the LSM scheme.

In previous LSM parameter calibration efforts, various sensitivity analysis methods have been applied. A commonly applied method, and the chosen method for this study, is the Sobol sensitivity method based on variance decomposition i.e. the variance contributed by each parameter to the total variance between model output and validation data is estimated (Sobol, 1993). The Sobol method has proven to generate valid results in previous LSM parameter sensitivity studies e.g., Chaney et al. (2016); Rosero et al. (2010); Hou et al. (2015). In a comparative study of global sensitivity analyses Tang et al. (2007) concluded that Sobol is the most effectively global alternative in disclosing first and total order parameter sensitivity.

The Sobol methodology is based on computerized mathematical techniques referred to as Monte Carlo simulations. In short, Monte Carlo simulations are applied to sample multiple sets of input data on which the model is run – one simulation for each generated set of model inputs. In the context of this study, a model input refers to a unique combination of parameter values on which the model is run. By analysing how the variance of simulated outputs varies when different parameter values are applied the variance contribution of each parameter is estimated by probability statistics (Saltelli, 2008). Emery et al. (2016) state that the main drawback of applying the Sobol methodology of complex models is the high computational cost due to the numerous simulations required for the results to be statistically significant.

2.3.2 Calibrating parameters

Much like in the sensitivity analysis, parameter calibration involves multiple model simulation. In this step, however, different values for parameters are tested with the objective to find what parameter values generate the least amount of output bias in relation to validation data. These parameter values for these simulations are preferably sampled with the Latin Hypercube sampling technique (Chaney et al., 2016; Hou et al., 2015). This is as Latin Hypercube sampling is a stratified sampling technique that efficiently explores the full range of possible parameter combinations. With this approach the number of sampled parameter sets is reduced which in turn reduce the number of necessary simulation. The number of possible parameter value combination increases exponentially with every additional parameter included in the calibration process. Consequently, the computational cost – both in terms of demand on computer and time resources – as well increases exponentially as all these parameter combinations are to be simulated. As such, reducing the number of parameters to calibrate by only including those identified as top most sensitive is preferable to enable as few parameter combination samples as possible.

3 Data

This section is devoted to the presentation of the data applied in the experiments and the characteristics of the study areas.

3.1 FLUXNET

Data used to validate LE and H simulation outputs and atmospheric data used to force simulations was collected from the FLUXNET network of micro-meteorological observation sites. At the present, FLUXNET include over 900 sites situated in terrestrial ecosystems of various environmental characteristics across 5 continents (Baldocchi et al., 2017). Observations include surface-atmosphere interface exchanges of carbon dioxide, water vapour and energy as well as meteorological, vegetation and soil data. FLUXNET data is commonly applied in LSM development e.g. Chaney et al. (2016) for the Noah LSM; Blyth et al. (2010) for Jules LSM; Joetzer et al. (2015) for ISBA.

3.2 Data selection

The selection of FLUXNET sites from which data was collect was based on a set of criterions. First, as governed by the study objective only forest areas with seasonal snow cover were sought after. This is as to continue the development of ISBA-MEB's ability to simulate the land surface energy fluxes in forest areas that was conducted by Napoly et.al (2016). Second, as ISBA-MEB (and LSM in general) is designed to simulate a broad spectrum of different environments at various temporal and spatial scales, parameter schemes need to be optimized accordingly. Thus, sites with varying vegetation and climate classifications were sought after. Third, a minimum observation time period criteria was set to three years of consecutive measurements. This is due to the models demand on "spin-up" (the model initially need some time to stabilize the simulated variables) as well as to have an adequate subsequent validation period. Other than these three main requirements there is also a forth data quality criterions relating to energy closure which is further discussed in section 3.3. Only four FLUXNET sites conforming to these criterions was found and used as study areas. These are described in the following sections and their main characteristics summarised in Table 1.

3.2.1 Tumbarumba forest

This Australian flux station is situated in the Bago State Forest of the southern tablelands of New South Wales (Lat/Lon: -35.6557 / 148.1521, 1200 m a.s.l). It is an open wet sclerophyll evergreen broad-leaf forest dominated by mature Alpine Ash (*Eucaluptus delegatensis*). Trees are mixed-aged up to 90 years with a mean canopy height of 40m and LAI of 2.87 m^2 m^{-2} (Keith et al., 2009). The understory is composed of grasses, herbs and 0.5 – 2 m shrubs. This 50000 ha forest is regenerating from over 100 years of selective wood production which came to a halt some 30 years prior to installation of the flux station in 2000. The climate is cool, moist temperate sub-alpine with mean annual temperature of 8 °C, mean annual minimum of 5.3°C and mean annual maximum of 19.5°C (Karan et al., 2016). Mean annual precipitation (MAP) is 1000 mm. Snowfall is common during the winter season and remains at the ground for 3 – 4 weeks. The soil class is acidic, eutrophic, red dermosol with moderate carbon and nutrient storage (Leuning et al., 2005). The soil in the study area never freezes.

3.2.2 Tharandt forest

This station is situated on a gentle south facing slope in the eastern part of a 60km^2 forest area, near the city of Tharand, 25 km SW of Dresden, Germany (Lat/Lon: 50.9624 / 13.5652, 380 m a.s.l.). It is an Evergreen Needle-leaf forest dominated by spruce trees (*Picea abies* and *Pinus sylvestris*) established by shedding in 1887, with tree density of 477 trees ha $^{-1}$, LAI of 7.6 m^2 m^{-2} and mean canopy height of 26.5 m (Grüwald & Bernhofer, 2007; Schwärzel et al., 2009). The understory consists primarily of young wavy Hair-grass (*Deschampsia flexuosa)* and European beech (*Fagus sylvatica)*. Apart from 1 ha open area mainly covered by grass to the west and 0.5 ha of laboratory buildings to the north, the area within the vicinity of the flux station is homogeneous with respect to vegetation characteristics. The climate is classified as warm temperate sub-oceanic fully humid with warm summers. Mean annual, maximum and minimum temperatures of 8.2 °C, 9.4 °C and 6 °C, respectively. Annual precipitation is 843 mm and snow covers the ground for about 72 days per year (European flux database, 2017).

3.2.3 Blodgett Forest

This site is situated adjacent to the University of California, at Berkley's Blodgett Forest Research Station on the western slope of Sierra Nevada Mountains, USA (Lat/Lon: 38.8953 / -120.6328, elevation 1315 m a.s.l). It is a 1200 ha flat ponderosa pine (*Pinus ponderosa*) plantation established in 1990, classified as mixed evergreen coniferous forest. The planted species is evenly aged at 7 – 8 years; with mean canopy height of 4m occupy over 70% of the total areal biomass in 1999 (Goldstein et al., 2000). The understory consist primarily of Whitethorn (*Ceanothus cordulatus*) and Manzanita (*Arctostaphylos*) shrubs. From mid-May to mid-June in 2000 there was a pre-commercial thinning removing all shrubs and ~60% of the trees, thereby decreasing the total LAI from ~7 to ~1m^2 m^{-2} (Fares et al., 2010). The climate is Mediterranean with hot, dry summers and cold, wet winters. Mean annual temperature is 11.9 °C and mean annual precipitation is 1630 mm (2540 mm snow) mainly falling between September and May, with almost no precipitation in the summer.

3.2.4 Harvard forest

Data is collected in the Prospect Hill tract approximately 100 km west of Boston, Massachusetts, USA (Lat/Lon: 42.5378 / -72.1715, elevation 340 m a.s.l). Surrounding the station is a moderately hilly mixed Deciduous Broad-Leaf forest dominated by 50 – 70 year old Red Oak (*Quercus rubra*) and Red Maple (*Acer rubrum*), with a mean canopy height of 23 m (Urbanski et.al, 2007). Three leaf emergence averages around day 140 and when fully grown the LAI of the site is 3.5m^2 m^{-2} (Freedman et al, 2001; Goldstein et al, 1998). The climate is humid continental with warm-summers and the average annual air temperature is 7.1 °C, average minimum of -12 °C in January and average maximum of 19 °C in July. Annual precipitation averages at 1071 mm, falling relatively evenly throughout the year.

Table 1. *Study areas characteristics. All data is collected from literature sited in the site description*

Site	**Tumbarumba**	**Tharandt**	**Blodgett**	**Harvard**
Country	Australia	Germany	USA	USA
Site Code	Au-Tum	De-Tha	Us-Blo	Us-Ha1
Study period	2001 – 2003	2002 – 2004	1999 – 2001	1992 – 1994
Latitude	-35.6566	50.9624	38.8953	42.5378
Longitude	148.1517	13.5652	-120.6328	-72.1715
Tower Height (m)	70	42	12.5	30
Forest type	Evergreen Broad-leaf	Evergreen Needle-leaf	Evergreen Needle-leaf	Deciduous Broad-leaf
Elevation m a.s.l	1200	380	1315	340
Climate classification (KGCC)	Cfb - Warm temperate fully humid with warm summer	Cfb - Warm temperate fully humid with warm summer	Csb - Warm temperate with dry, warm summer	Dfb - Warm Summer Humid Continental
Mean annual Temperature (°C)	8.0	8.2	11.1	7.1
Mean annual precipitation (mm)	1000	843	1226	1071

3.3 Validation data

Validation data consist of 30 minutes average LE and H fluxes measure by eddy covariance sensors mounted on micrometeorological towers. Eddy covariance is a method for computing vertical net flux transported by eddys at the physical point of the sensor in a given times unit. Eddy covariance is considered as the most reliable method for this particular application (Baldocchi et al, 2001). However, the method is associated with the well-known energy closure imbalance issue (Majozi et al, 2017*)*. The first law of thermodynamics (i.e., the law of conservation of energy) state that energy can neither be created nor destroyed – only transformed from one form to another. Thus, energy absorbed by the land surface must be partitioned into emission of equivalent quantity. This issue is often described using a rewrite of the energy balance equation presented earlier:

$$Rn - G = H + LE \tag{2}$$

The energy closure issue arises as energy quantity of turbulent fluxes (right hand side of equation) measured by eddy covariance systems are not equivalent to the amount of the Rn minus the amount of energy emitted to the soil (left hand side of equation). Studies show that the general closure imbalance for eddy covariance FLUXNET sites is 10 – 30 % (Wilson et al, 2002). To use validation data with minimum bias only data from sites with energy closure imbalance less than 10 % was included.

3.4 Atmospheric forcing data

Forcing data include incoming short-wave radiation intercepted directly from the sun, incoming short-wave radiation scattered by the atmosphere, incoming long-wave thermal radiation, separate rain and snow precipitation, wind speed, wind direction, air temperature, air specific humidity, atmospheric pressure and atmospheric CO^2. This data had been recorded by various specialized sensors and tools mounted on meteorological towers and on the ground either on or adjacent to the eddy covariance towers where the flux data was recorded. All forcing data represent 30 minutes average values.

3.5 Physiography parameters

Data used to provide the LSM with information on physiography of the land surface through numerical parameterisation was collected from three sources; databases, literature and estimations. The majority of parameters were prescribed by coupling the LSM to two different databases. Vegetation related parameters were derived from ECOCLIMAP database which is a SURFEX native global, 1km spatial resolution land cover database with 550 land cover types (Masson, 2013). These cover types are composed by satellite data and land cover maps. For parameters representing soil characteristics the model was coupled to the Harmonized World soil Database (HWSD). This is a global 30 arc-second raster database composed of regional and national soil information with information from the FAO-UNESCO Soil Map of the World database (FAO, 2017).

Parameter values derived from databases are however generalized relative to the spatial resolution. Therefore, a literature study was conducted to find site specific parameter values relevant for the given study periods. In the instances when adequate such data was found for all four sites this data had power over the data base values. The main parameters are summarized in Table 2.

3.6 Initial state variables

Besides forcing data and parameter prescriptions the model also need to be provided with the initial state of some variables such as soil water and ice content, soil temperature, snow density, snow thickness and snow temperature. Prescription values for initial parameters that was not disclosed in the reviewed literature, supplied by FLUXNET or included in the databases were estimated by “spin-up” simulations. Here, spin-up simulation refers to the process of simulating the target area without knowing the initial state variables and letting the model simulate an estimated value for that variable (Carrer et al, 2013). For each site, this was performed by defining all parameter and initial state variables that were known in the model scheme. The model was then run for nine years forced with this available three years of forcing data multiplied by three. During the simulation the sought after state variables are simulated based on the evolution of the land surface. The last state variable value of the first day of the last simulated year was then used to represent the initial state of each estimated variables in the subsequent simulations. Several such simulations were conducted whereupon nine years of spin-up period was identified as adequate.

Table 2. *Values used to prescribe the main ISBA-MEB vegetation and soil parameters for the four forest study areas. The source column indicates that data is either based on database coupling or values found in the literature cited in the study area description section.*

Site	**Tumbarumba**	**Tharandt**	**Blodgett**	**Harvard**	**Source**
Soil Parameters					
Sand (%)	54	37	42	76	*HWSD*
Clay (%)	27	23	29	8	*HWSD*
Soil Organic Carbon 0-30 cm (kg/m^2)	3.5	3.2	5.6	5.8	*HWSD*
Soil Organic Carbon 70-100 cm (kg/m^2)	3.9	4.0	5.6	7.9	*HWSD*
Soil depth (m)	*5*	3	3	3	*ECOCLIMAP*
Root Depth (m)	*5*	2	2	2	*ECOCLIMAP*
Soil albedo mean y^{-1} Visible / Near infrared (Reflectance fraction in %)	0.089 / 0.22	0.079/0.19	0.071/0.19	0.085 / 0.23	*ECOCLIMAP*
Vegetation Parameters					
Total LAI (m^2 /m^2)	2.87	7.6	7.1 in 1999 1.2 in 2001	0.3 day 110 to 3.5 day 180	*Literature*
Mean Canopy Height (m)	40	26.5	4	23	*Literature*
Vegetation albedo mean y^{-1} Visible / Near infrared (Reflectance fraction in %)	0.029 / 0.187	0.025/0.137	0.029/0.175	0.040/0.230	*ECOCLIMAP*
Vegetation fraction (%)	0.95	0.95	0.95	0.95	*ECOCLIMAP*
Ground litter (cm)	3	3	3	3	*ECOCLIMAP*

4 Method

In this section the pre-processing of model input data and the model setup is first described followed by description of the applied sensitivity analysis and parameter calibration.

4.1 Data quality control

Data distributed by FLUXNET is pre-processed according to harmonized standards including gap filling of missing data and partitioning (Chaney et al., 2016). Nonetheless, additional quality control was conducted to minimize data uncertainty. Forcing and validation data time series were inspected to ensure no missing values and that the data followed the annual and seasonal cycles as well as to identify outlier values. No missing values were found but a handful of illogical outliers in the forcing data were identified and substituted for interpolated values.

4.2 Model set up

As discussed in section 2.2.2, ISBA-MEB enables separation of the land surface into three distinct fully coupled energy budgets and all simulations un this study the model was set to separate the ground, the canopy and snowpack into distinct energy budgets. Ground heat transfers were modelled using a diffusive soil (DIF) option which mean that the ground is divides into 15 layers exchanging energy amongst each other and with the surface (Decharme et al., 2011).ISBA- MEB incorporate a multi-layer canopy option that models what fraction of incoming radiation is intercepted by the canopy, what fraction is transmitted to the ground and how much is reflected (Carrer et al., 2013). As the modelled forest areas have seasonal snowfall the snowpack was treated with the ISBA Explicit Snow Processes (ISBA-ES) which is an multi-layer option that separate the snowpack into 12 layers (Decharme et al., 2016). This approach enables representation of different temperature, density and water equivalent content in the different sections of a snowpack. During simulations the model was supplied with 30 minute atmospheric forcing during the three years of modelling time. The model was run on a single point in space representing the footprint of the micro-meteorological tower from which the forcing and validation data was collected. To match the validation data the model was set to output 30 minutes average flux values over the course of the three year simulations.

4.3 Parameter calibration

As discussed on section 2.3 the applied parameter calibration methodology includes a Sobol sensitivity analysis to explore parameter sensitivity followed by the actual calibration of parameters identified as highly sensitive. Both the sensitivity analysis and the subsequent calibration process are based on multiple runs of the same model in which the parameters are prescribed to statistically sampled values. Multiple model runs is here forth referred to as simulation iterations, a set of sampled parameter values applied in one simulation iteration is referred to as a parameter vector and a collection of such vectors is referred to as a sample matrix. The Sobol methodology was selected as it has shown to generate the best results in previous LSM parameter sensitivity studies. Parameter values for the simulation iterations in the calibration step is sampled with the Latin Hypercube Sampling technique as this approach has proven to be effective and reliable in previous parameter calibration studies.

Algorithms were implemented in Python and Bash including the python sensitivity analysis packages SALib (Herman & Usher, 2017) and the SciPy stack for numerical and statistical data processing (van der Walt et al., 2011). ISBA-MEB itself is written in Fortran90 and simulations were performed on a computer cluster of the National Supercomputer Centre at Linköping University.

4.3.1 Sensitivity analysis

The concept of sensitivity analysis has been described by Saltelli (2008) as the study of how uncertainty in the output of a model can be apportioned to different sources of uncertainty in the model inputs. In the context of this study those inputs are the model process parameters. Sobol sensitivity analysis is a statistical variance-based approach belonging to a class of probabilistic approaches used to quantify model input and output uncertainty as probability distributions (Sobol, 1993). The core of this methodology is variance decomposition which is a way to apportion the total variance between simulated and validation data into parts attributable to input factors and combinations of these factors. This is achieved by running multiple simulation iterations on different parameter vectors and evaluating how the variance of the model output varies as parameter values are varied.

In practice, this approach includes four main steps. 1) Selecting a set of parameter to include in the analysis i.e. parameter candidates. 2) Sampling a matrix of parameter vectors that will be used to prescribe the parameters in each of the simulation iterations. 3) Run the model once for each parameter vector and quantify the variance between the simulated output and the validation data. 4) Decompose the total variance into parts attributable to each parameter.

4.3.2 Parameter candidates

In theory, with unlimited resources the sensitivity of all model parameters could be evaluated. However, ISBA-MEB is a highly non-linear and computational demanding model including numerous parameters and the computational cost of the Sobol algorithm increases exponentially for every additional included parameter – thus such an approach would seem ill advanced. Furthermore, just like in nature certain land surface components and ecosystem processes influence turbulent fluxes more than others. Testing the sensitivity of all model parameters for a limited amount of output variables would therefore be theoretically irrelevant. An intermediate approach is instead to select a set of parameter candidates with strong coupling to the target variables (Chaney et al., 2010). Consequently, this selection must be based on firm knowledge of the physical meaning of the parameters and how this is implemented in the model structure. In the parameter candidate selection process the emphasis was therefor on parameters that influence turbulent fluxes and this selection was performed in consultation with SURFEX developers and researchers at SMHI and Météo France (Table 3).

Table 3. *Parameter candidates. Min and max columns denote the lower and upper bound of the ranges within which parameter values were varied during the sensitivity analysis and parameter calibration.*

Name	***Physical meaning***	***Min***	***Default***	***Max***
XTAU_LW	*Longwave radiation transmission factor* Parameter included in the computation of the 'view-factor' i.e. the proportions between the amount of sky and vegetation that is visible from a particular point on the ground (Boone et.al, 2016). This proportion is directly related to the amount of radiation the canopy and the ground is exposed to as well as how much energy can leave the forest. Adjusting this parameter alters the proportions of the view-factor. Previous studies have concluded that the default value of 0.5 is to be used, but little is known of how this factor may differ between environments.	0.4	0.5	0.6
XUNIF_CV	*Vegetation/soil heat-capacity* Parameter included in algorithms computing the heat capacity of vegetation and soil (Boone et.al, 2016). Heat capacity plays a key role in estimating heat flows between soil, vegetation and the atmosphere. This parameter is known to be uncertain and little is known of how this parameter is to be prescribed in different forest environments.	0.5E-5	1.0E-5	2.0E-5
Z0m/Z0h	*Ratio Z0m/Z0h* ZOm denotes the roughness length of momentum i.e. the height above the land surface where the wind speed reaches zero due to friction of the surface. ZOh denotes the thermal roughness length i.e. the distance between the land surface and a point above that surface where the temperature is the same. There is a relationship between these two and as it is easier to estimate ZOm it is used estimate ZOh in the present model setup. This parameter denotes the ratio between these phenomena. There is currently an active debate of how the default value of this parameter is to be prescribed in different forest environments.	1	10	10
XXB_SUP	*Sigma parameter in clumping index (canopy top)* Clumping refers to the density of leafs and the clumping index is used as a measure of the dispersion/grouping of canopy leaves. Carrer et.al (2013) found that ISBA simulated carbon fluxes are sensitive to this parameter and as leaf structure affects incoming and outgoing turbulent fluxes in forests it is relevant to evaluate how sensitivity LE and H fluxes are to this parameter. This parameter defines the clumping index of the canopy top but clumping index at canopy bottom is also included as a parameter candidate. Carrer et.al (2013) found the canopy top parameter to be more sensitive than the canopy bottom. This property differs between tree species and thus the default values and ranges are vegetation specific.	Default/2	Au-Tum: 3 De-Tha:2 Us-Blo:2 Us-Ha1:1	Default * 2
XXB_INF	*Sigma parameter in clumping index (canopy bottom)* The definition of clumping index is described in XXB_SUP along with the motivation to analyse it. This parameter defines the clumping index at canopy bottom which is found by Carrer et.al (2013) to be less sensitive than clumping index at canopy top. This property differs between tree species and thus the default values and ranges are vegetation specific.	Default/2	Au-Tum: 4 De-Tha: 2 Us-Blo: 2 Us-Ha1: 4	Default * 2
XGT_SUP	*Leaf orientation parameter (canopy top)* This parameter defines the angular orientation of leafs at canopy top. This property affect the amount of radiation intercepted or absorbed by leafs as well as how much radiation penetrates the canopy. Carrer et.al (2013) found that ISBA simulated carbon fluxes are sensitive to this parameter and as leaf orientation affects incoming and outgoing turbulent fluxes of a forest it is relevant to test how sensitivity LE and H fluxes are to this parameter. Carrer et.al (2013) found this canopy top parameter to be more sensitive than the corresponding canopy bottom parameter.	0.4	0.5	0.6
XGT_INF	*Leaf orientation parameter (canopy bottom)* The definition of leaf orientation is described in XXB_SUP along with the motivation analyse it. This parameter defines the leaf orientation at canopy bottom which is found by Carrer et.al (2013) to be less sensitive than leaf orientation at canopy top.	0.4	0.5	0.6

4.3.3 Parameter sampling

Sampling can be thought of as a tool to explore a domain of interest. In the context of this study the domain of interest is the possible values within the specified parameter ranges i.e. the parameter space. The exploration is conducted by testing the outcome of running the model with parameters prescribed to different values drawn from the parameter space.

In accordance with the Sobol method the sampling matrix was generated by the Saltelli sampling technique (Saltelli, 2008). This approach is conducted by first generating a matrix of parameter vector referred to as the base sample. This matrix is sampled using the Sobol quasi-random sampling techniques (i.e. Sobol sequence) designed to generate uniformly distributed parameter samples in more uniform way than simple random sampling. This is achieved by avoiding sampling previously sampled values and by doing so avoid sampling clusters and gaps in the parameter space. The Saltelli extension is then applied by "cross-sampling" the base sample by holding one parameter value of a base sample parameter vector fixed at a time while generating samples for the rest of the vector values.

Due to the computational cost of Monte Carlo simulations it is relevant to use techniques to generate as low number of sampling vectors as possible. However, as the Sobol method is based on probability theory, for the derivatives to be statistically significant the sample must at the same time be representative for the whole parameter space. The number of samples necessary to fulfil these requirements is dependent on, and increases with model complexity and the number of parameter included in the analysis but other than these factors there is no general consensus in how many vectors to sample (Zhang et al., 2013). To evaluate the appropriate sampling size several sample matrices was generated holding 160 to 3840 vectors on which the model was iterated. The validity of these simulation results was then evaluated by inspecting how the derived parameter sensitivity varied between matrices. These tests revealed that patterns in sensitivity varied with matrices of less, but not more than 2560 vectors. This sampling size was therefor used for the subsequent sensitivity analyses. Investigations were also conducted to evaluate if aggregating the original 30 minutes time series data into 6, 12 and 24 hour time step affected the parameter sensitivity estimates; this was indeed the case and therefor the 30 minutes time step was selected to achieve optimal accuracy.

4.3.3 Sensitivity iterations

For each forest site, the model was iterated once for each sampled parameter vector. To match the validation data the model was defined to output time series of 30 minutes average turbulent H and LE fluxes over three year periods. As the Sobol approach is a variance based method it is not the model output time series itself that is analysed, but the variance between the model output and the validation data time series. The first year of simulated was considered model spin-up and thus only the last two years were used in the comparison. The Mean Square Error (MSE) objective function was applied to quantify variance which is written as:

$$MSE = \frac{\sum_{i=1}^{k}\left(O_{sim,i} - O_{obs,i}\right)^2}{k} \quad (3)$$

where k is the total number of simulated time steps, $O_{sim,i}$ is the simulated output at time i and $O_{obs,i}$ is the observed value at that same time i. This measures squared mean of all 30 minutes time steps. LE and H variables were processed separately.

4.3.4 Analysing sensitivity

A simulated output variable of any mathematical model can be expressed as a function:

$$Y = f(X_1, X_2, X_3, \dots, X_n) \tag{4}$$

where Y is the model output, X_1, X_2 and X_3 are factors included in the computation of the model output and X_n denotes the total number of included factors. In the context of this study the model output is either LE or H and the factors are the parameters.

With variance decomposition the aim is to find out what would happen to the variance of Y if the true value of a factor X_i were to be found and by doing so discern that factors variance contribution to the total variance. Variance decomposition is expressed as:

$$Var(Y) = \sum_{i} V_i + \sum_{i<j} V_{ij} + \sum_{i<j<k} V_{ijk} + V_7, \dots, n \tag{5}$$

where $Var(Y)$ denotes the total variance of the output variable – this is the previously computed MSE. V_i is denoted the first order variance index which is an estimate of the variance contribution of X_i to $Var(Y)$ not accounting for interactions with other factors. V_{ij} denotes the second order variance index which is interpreted as the sum of the first order variance contribution of X_i and the variance due to this factors interaction to a second factor X_j. Higher order variance indices can be computed for interactions amongst all analysed factors n as well as the total order index which is an estimate of the variance contribution of all factors but X_i.

To decrease the computational cost of the algorithm, often only the first and total order variance is computed. Deriving only these two indices is adequate to fulfil the objective of this study. The first order and total order indices are estimated as:

First-order variance index

$$V_i = Var[E(Y|X_i)] \tag{6}$$

Total-order variance index

$$V_{\sim i} = Var[E(Y|X_{\sim i})] \tag{7}$$

In the equation for the first order variance contribution $E(Y|X_i)$ is the conditional expectation i.e. the expected value of Y when it is estimated based on the sampled values for factor X_i. $Var[E(Y|Xi)]$ is then the variance of the condition expectations calculated of all sampled values for factor X_i. If this variance is big then the influence of that factor is important. In the equation for calculating the total order variance contribution $X_{\sim i}$ denotes all parameters except

X_i - hence the total variance contribution measures how much variance would be left if the true values of all parameters but X_i were known. With these estimates the first and total order sensitivity indices can be estimated as:

First-order sensitivity index:

$$S_i = \frac{V_i}{Var(Y)} \tag{8}$$

Total-order sensitivity index:

$$S_{Ti} = 1 - \frac{V_{\sim i}}{Var(Y)} \tag{9}$$

where S_i measures the main effect (i.e., individual sensitivity) of a factor X_i, $V_{\sim i}$ denotes the amount of variance contributed by all factors but X_i and therefor S_{Ti} is a measurement of the sum of S_i of X_i and the higher order interactions of X_i with all other factors. The numerical value of a factors S_i denote the fraction of the total sensitivity apportioned to that factor i.e. a parameter with S_i 0.8 constitutes 80 % of the sum of all parameters S_i. The sum of all parameters S_i should therefore theoretically be 1. As S_{Ti} represent S_i plus all higher order indices, the sum of S_{Ti} should theoretically be 1 or more.

It was these sensitivity indices that were used to discern how sensitive the model is to each of the parameter candidates. Those parameters associated with the highest sensitivity were then subjects of the calibration. Interpreting sensitivity indices to discern what parameters are associated with significant uncertainty is subjective. Chaney et al. (2016) and Hou et al. (2015) interpret parameters apportioning at least 10 % of the total sensitivity at a site as highly sensitive. Based on these premises three parameters were classified as highly sensitive and was therefore analysed in the subsequent calibration process. For further elaboration and discussion of this sensitivity methodology see Saltelli (2008), in particular chapter 1 and 5.

4.3.5 Calibrating parameters

The calibration process is conducted by iterating the model on sampled parameter vectors and adopting the values of the vector that generate the least amount of variance between simulated and observed values as the optimal set of parameters. Reducing the amount of parameters to calibrate by only including those most sensitive ensure calibration of relevant parameters and reduces the computational cost of the calibration process. For further efficiency the stratified Latin Hypercube sampling technique was applied to generate the sampling matrix for the calibration iterations. Latin Hypercube sampling divides (i.e., stratifies) the parameter probability space into subgroups (i.e., stratum) of equal proportion and then randomly samples an equal amount of samples from each stratum. By doing so the whole parameter space is effectively represented. Chaney et.al (2016) found it adequate generate 1000 Latin hypercube sample for calibrating three parameters and this approach was adopted in the present study i.e. 1000 unique parameter sets are generated for each forest site for a total of 4000 model runs.

The performance of each vector was defined as the sum of the normalized LE and H variance quantified by Normalized Root Mean Square Deviation (NRMSD). Starting by computing the root mean square deviation of both LE and H separately, the cost function is written in three steps as:

$$RMSD = \sqrt{\frac{\sum_{i=1}^{k}\left(O_{sim,i} - O_{obs,i}\right)^2}{k}} \tag{10}$$

where $O_{sim,i}$ is the simulated time series at each simulated times *i*, $O_{obs,i}$ is the observed time series at that same time *i* and *k* denote the total number of times steps. The RMSD is then normalized by division by the mean of the range i.e., the maximum value minus the minimum values of the observed data time series:

$$NRMSD = \frac{RMSD}{\max(O_{obs,i}) - \min(O_{obs,i})} \tag{11}$$

Finally, the NRMSD of the variables are summed for use as a performance metric of each parameter vector:

$$LE_{NRMSD} + H_{NRMSD} \tag{12}$$

5 Results

In this section the results of the parameter calibration process is presented.

5.1 Sensitivity analysis

The factional uncertainty contribution of the analysed parameter candidates to MEB LSM modelled turbulent LE and H fluxes was analysed by the Sobol methodology and quantified in terms of first order (S_i) and total order (S_{Ti}) sensitivity indices (Figure 5) – see section 4.3.4 for definitions of these indices.

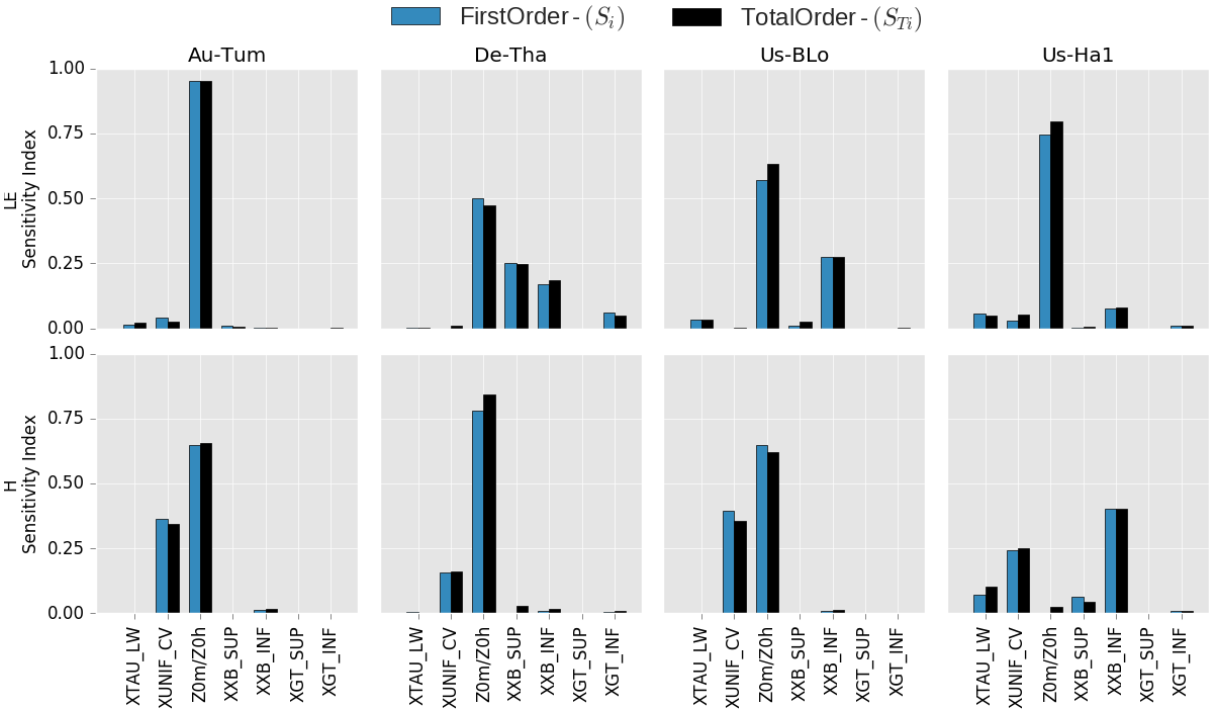

Figure 5. *Parameter sensitivity indices at the four forest study areas; Tumbarumba (Au-Tum), Tharandt (De-Tha), Blodgett (Us-Blo) and Harvard (Us-Ha1).Each of the eight diagrams illustrate the sensitivity index of tested parameters (outlined in Table 3) in relation to the tested turbulent latent (LE) and sensible (H) heat flux model output variables (rows) at each of the study areas (columns).The X-axis, which is shared by all diagrams, denotes the names of the analysed parameters and the Y-axis represents the fractional sensitivity measure of these parameters ranging from 0 to 1.*

The sensitivity analysis results indicated that the greatest parameter sensitivity is in general attributed the *ratio between roughness lengths of momentum and roughness lengths of heat* (Z0m/Z0h) for both LE and H at all four forest sites. Harvard forest (US-Ha1) however deviate from this pattern as both S_i and S_{Ti} of this parameter for H is neglectable. The second most sensitive parameter is XUNIF_CV representing the *heat capacity of vegetation and soil*. For LE the influence of this parameter is neglectable, but for H it is the second largest at all sites. The *sigma clumping index at canopy bottom* (XXB_INF) has relatively high sensitivity indices for LE at all sites except the Australian forest (Au-Tum). For H, this parameter was not estimated to be sensitive except for Us-Ha1 where it instead was estimated to be the most sensitive. The sensitivity of the *longwave radiation transmission factor* (XTAU_LW), *leaf orientation at canopy top* (XGT_SUP) and *leaf orientation at canopy bottom* (XGT_INF) parameters is in this context neglectable. The same applies for the *sigma parameter in clumping index at canopy top* (XXB_SUP) for all sites except for LE at the German forest

(De-Tha) where it instead is the second most sensitive parameter. The values S_{Ti} do not deviate remarkably from S_i which implies that even though there is higher order interactions amongst the tested parameters the main parameter sensitivity is due to the direct influence of these parameters on modeled outputs. Based on these results Z0m/Z0h, XUNIF_CV and XXB_INF is ranked as the top most sensitive parameters and were therefore subjects of the subsequent calibration process.

5.2 Parameter calibration

Similar to the sensitivity analysis, the calibration process was conducted by running multiple simulations in which parameter prescriptions were varied. In this step, the aim was to find the parameter prescription that generates the least amount of cumulative variance in simulated turbulent LE and H fluxes. The focus of this study is on calibrating parameters for simulation of LE and H. However, as components of the land surface energy budget, turbulent fluxes cannot be analysed in isolation but must be considered in the context of energy availability (i.e., Rn) and what proportion of this energy is conducted into the ground (i.e., G flux). Therefore, these four components are included in the analysis. In the following four sections simulated time series applying default and optimal parameter values are presented along with the corresponding observed time series for the individual study areas.

5.2.1 Tumbarumba forest

The Australian broad-leaf eucalyptus forest displayed pronounced diurnal cycles in all months (Figure 6). Simulated Rn correlates well with observations and the partitioning of this energy into LE and H is in general well represented throughout the year. However, for the three last months of the year both the default and the optimized parameterization overestimate LE and underestimate H. The optimal parameterization however decreases this bias which is reflected in the lower NRMSD of this simulation. The bias in the Gflux time series is too small to explain these errors and therefor source of this bias may be errors in input data. Overall, the optimisation process slightly decreased the variance between simulated and observed LE and H time series. These improvements slightly compensate the total bias.

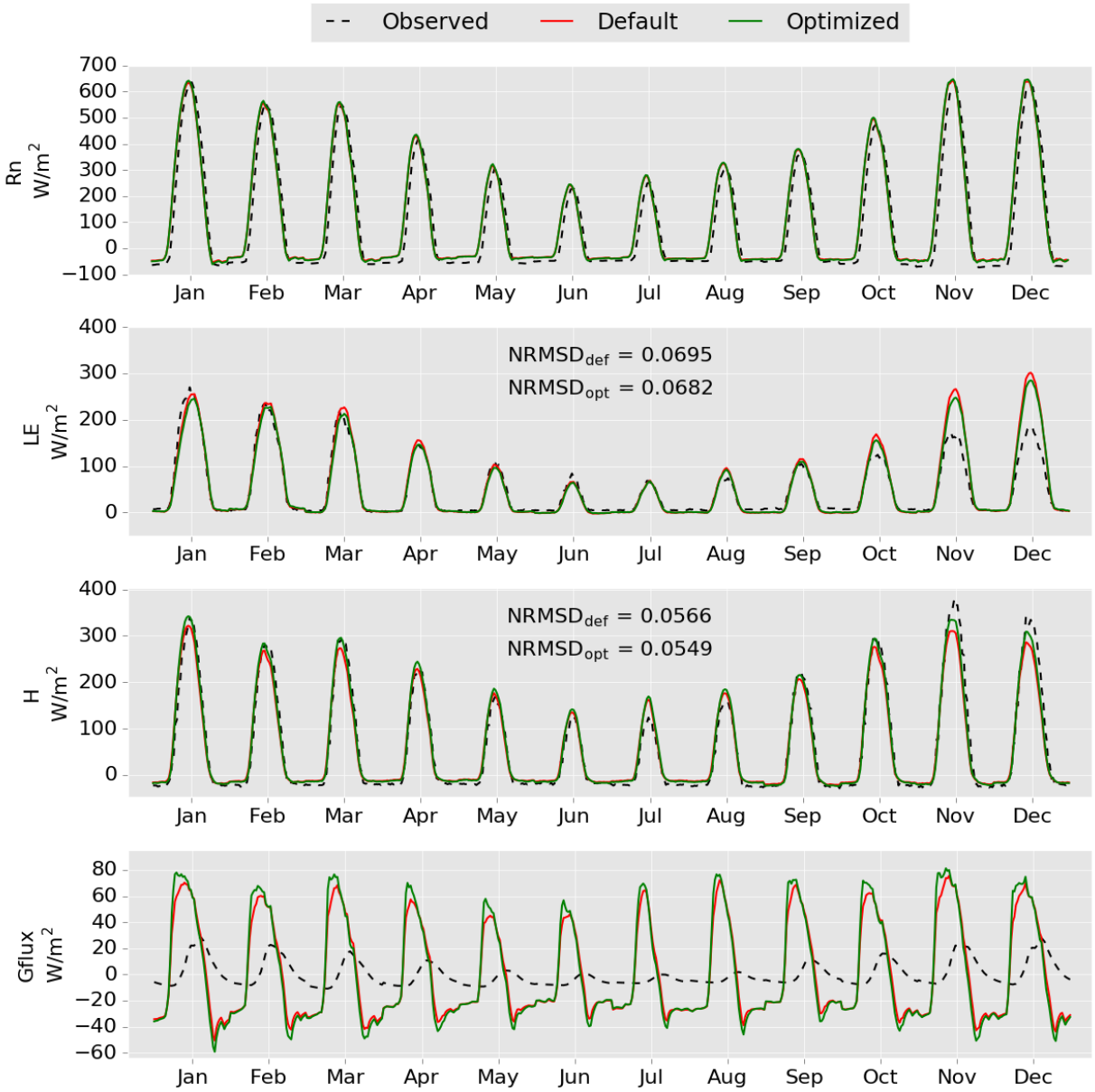

Figure 6. *Average monthly diurnal cycles of net radiation (Rn), latent (LE) heat flux, sensible (H) heat flux and ground heat flux (Gflux) at Tumbarumba forest (Au-Tum) in 2002 and 2003 simulated with default and optimized parameters. The performance of simulation with default parameters and optimized parameters is expressed in Normalized Root Mean Square Deviation (NRMDS) from observed values for the variables to which parameters are calibrated.*

5.2.2 Tharandt forest

Rn at this German Evergreen Needle-leaf forest is in general well represented for both the default and the optimised simulation, but the energy partitioning is not adequate (Figure 7). A general day-time LE flux overestimate is disclosed for LE, especially for May to September. For H there is instead a general night-time underestimate. LE bias is marginally decreased in the optimised simulation whereas the bias for H instead increases. The fact that an optimized parameter set can actually result in greater variance for a variable is due to the definition of the cost function. Recall from section 4.2.5 that the cost is defined as the cumulative variance of LE and H. Consequently, as the variance decrease for LE is so great at this site, the variance increase of H is compensated. The bias in the Gflux time series is too small to explain these errors and therefor source of this bias may be errors in input data.

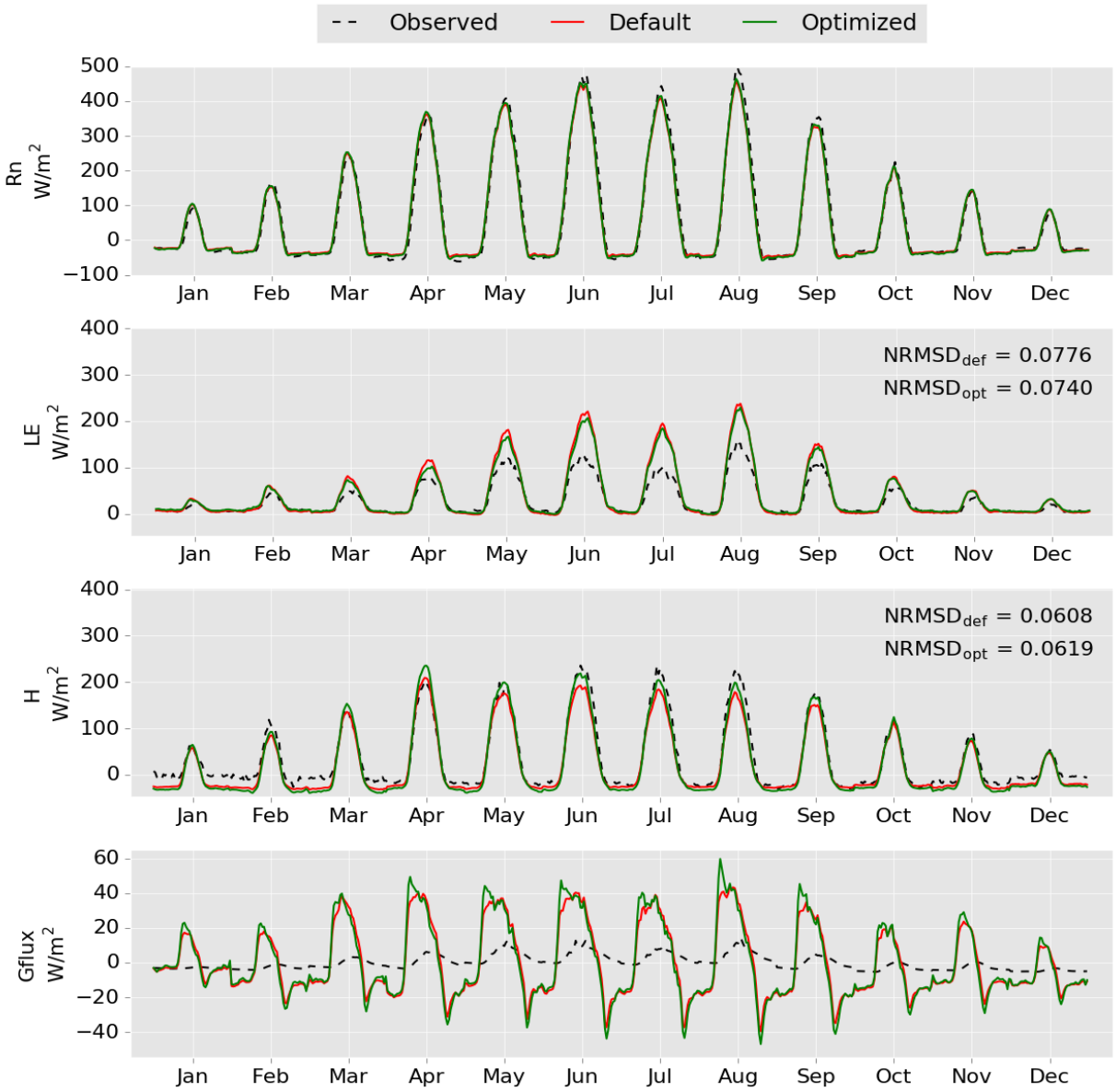

Figure 7. *Average monthly diurnal cycles of net radiation (Rn), latent (LE) heat flux, sensible (H) heat flux and ground heat flux (Gflux) at Tharandt forest (De-Tha) in 2003 and 2004 simulated with default and optimized parameters. The performance of simulation with default parameters and optimized parameters is expressed in Normalized Root Mean Square Deviation (NRMDS) from observed values for the variables to which parameters are calibrated.*

5.2.3 Blodgett forest

The simulated Rn at this Californian planted mixed evergreen coniferous forest is underestimated from May to November which consequently affects all other components of the energy budget system (Figure 8). This bias is reflected in flux underestimates for H in May and for LE from June to October. LE bias is especially great in June and August which is interpreted as a consequence of underestimated Rn and overestimations in H and Gflux. Marginal compensation for these biases is achieved by calibrating the parameters.

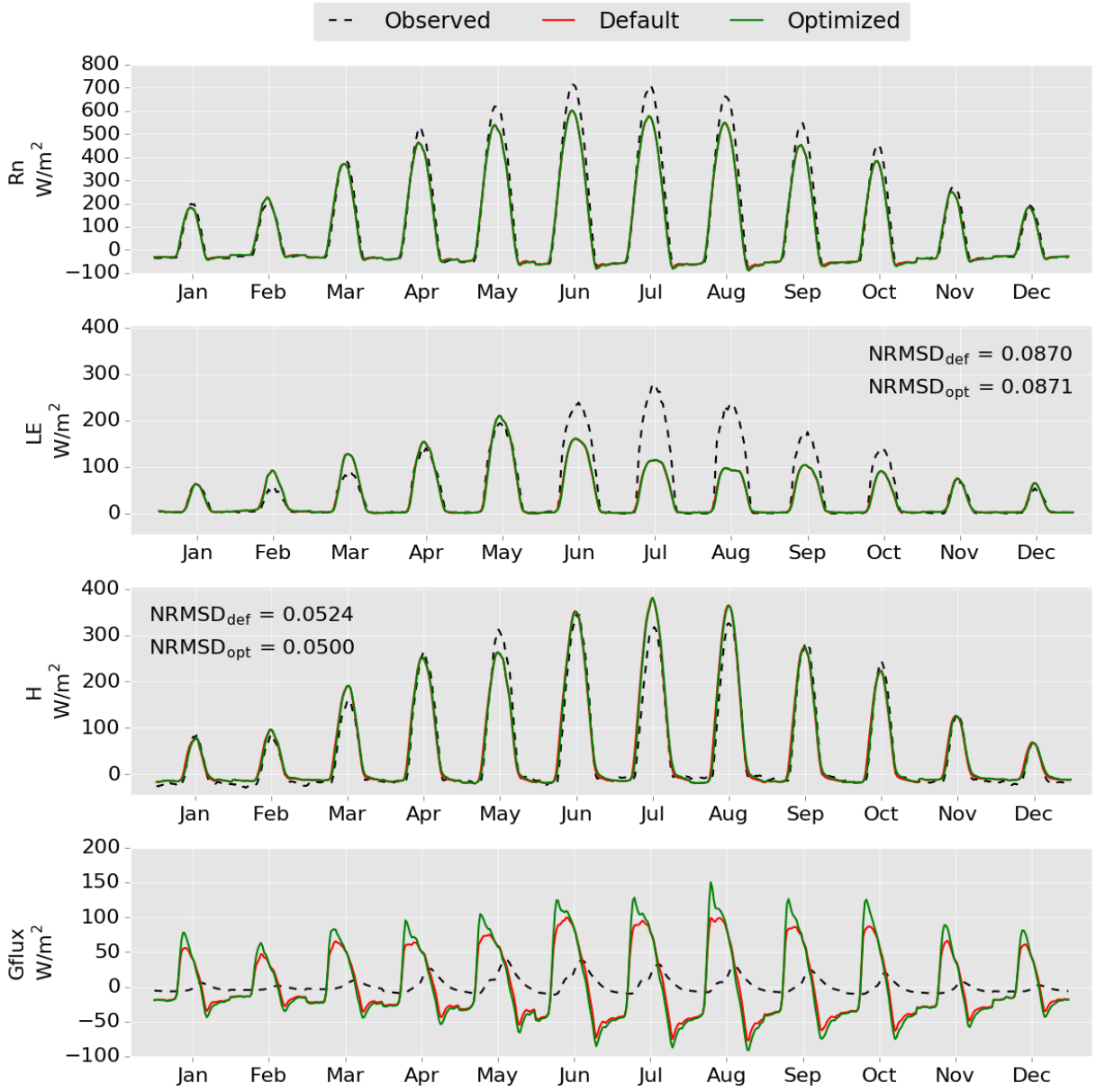

Figure 8. *Average monthly diurnal cycles of net radiation (Rn), latent (LE) heat flux, sensible (H) heat flux and ground heat flux (Gflux) at Blodgett forest (Us-Blo) in 2000 and 2001 simulated with default and optimized parameters. The performance of simulation with default parameters and optimized parameters is expressed in Normalized Root Mean Square Deviation (NRMDS) from observed values for the variables to which parameters are calibrated.*

5.2.4 Harvard forest

Simulated Rn is in general underestimated at this mixed Deciduous Broad-Leaf forest for both the default and optimal parameterization. This underestimate is especially tangible for the three first months of the year which consequently lead to great underestimate of H. In April and May Rn is however realistically simulated, but the partitioning of this energy skewed as LE is overestimated and H underestimated. In the diurnal cycles of the remaining months LE and H is in general slightly underestimated or overestimated. Overall the calibration marginally improves both LE and H simulation and simulated bias is greater during the first half year more than the second half. No observations of Gflux were available for this site.

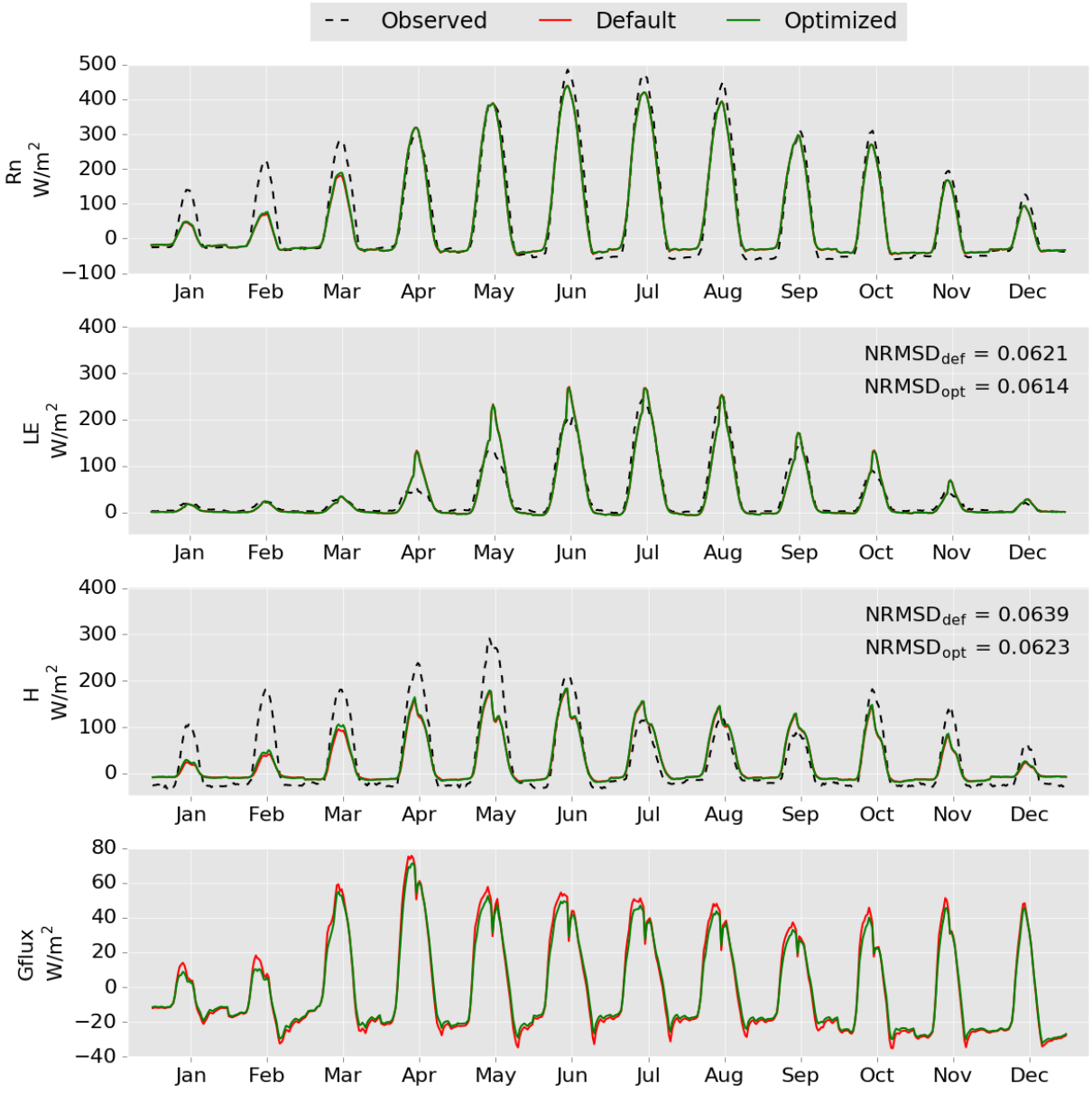

Figure 9. *Average monthly diurnal cycles of net radiation (Rn), latent (LE) heat flux, sensible (H) heat flux and ground heat flux (Gflux) at Harvard forest (Us-Ha1) in 1993 and 1994 simulated with default and optimized parameters. The performance of simulation with default parameters and optimized parameters is expressed in Normalized Root Mean Square Deviation (NRMDS) from observed values for the variables to which parameters are calibrated.*

5.2.5 Optimal parameter vectors

Calibrating the three top most sensitive parameters revealed the site specific optimal parameter values. The output variance of all simulations of the calibration iterations is plotted against the parameter values used in the corresponding simulations to identify patterns in variance as a function of parameter prescriptions (Figure 10). Parameter values generating the least amount of variance vary between sites. The majority of the values of the optimal vectors lie at the edges of the parameter range indicating that values outside these ranges would further decrease variance. Expanding the parameter ranges would however lead to unrealistic parameter prescriptions as such values would not be in accordance with the parameters physical meaning.

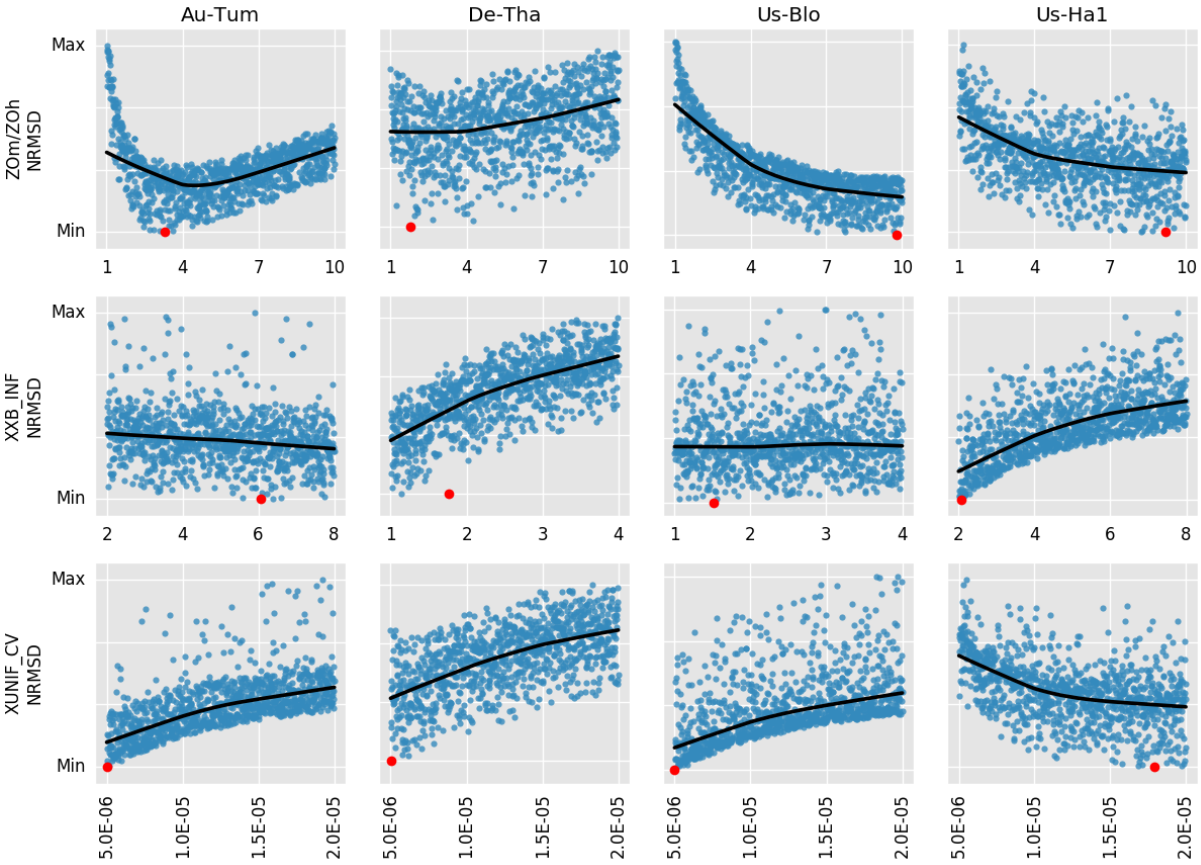

Figure 10. *Prescribed parameter values (outlined in Table 3) and resulting output variance of parameter calibration simulation iterations for forest study areas; Tumbarumba (Au-Tum), Tharandt (De-Tha), Blodgett (Us-Blo) and Harvard (Us-Ha1). In each of the 12 diagrams the Y-axis marks cumulative turbulent latent (LE) and sensible (H) heat flux Normalized Root Mean Square Deviation (NRMSD) from observed flux time series and the X-axis marks the range of tested parameter values. Blue dots mark a parameter value and the resulting variance of using that value in a simulation. Red dots mark parameter values identified to generate the least amount of simulated NRMSD. The black lines are intended as a visual aid to illustrate patterns in parameter values VS resulting variance.*

The optimized parameters reduce simulation bias by 0-2 Wm/^{2} for both LE and H at all sites but for H at De-Tha (Figure 11). In addition, model fit expressed in R^2 measuring how well simulated time series correspond to dynamic changes in observed data is also in general improved except for LE at Au-Tum and De-Tha.

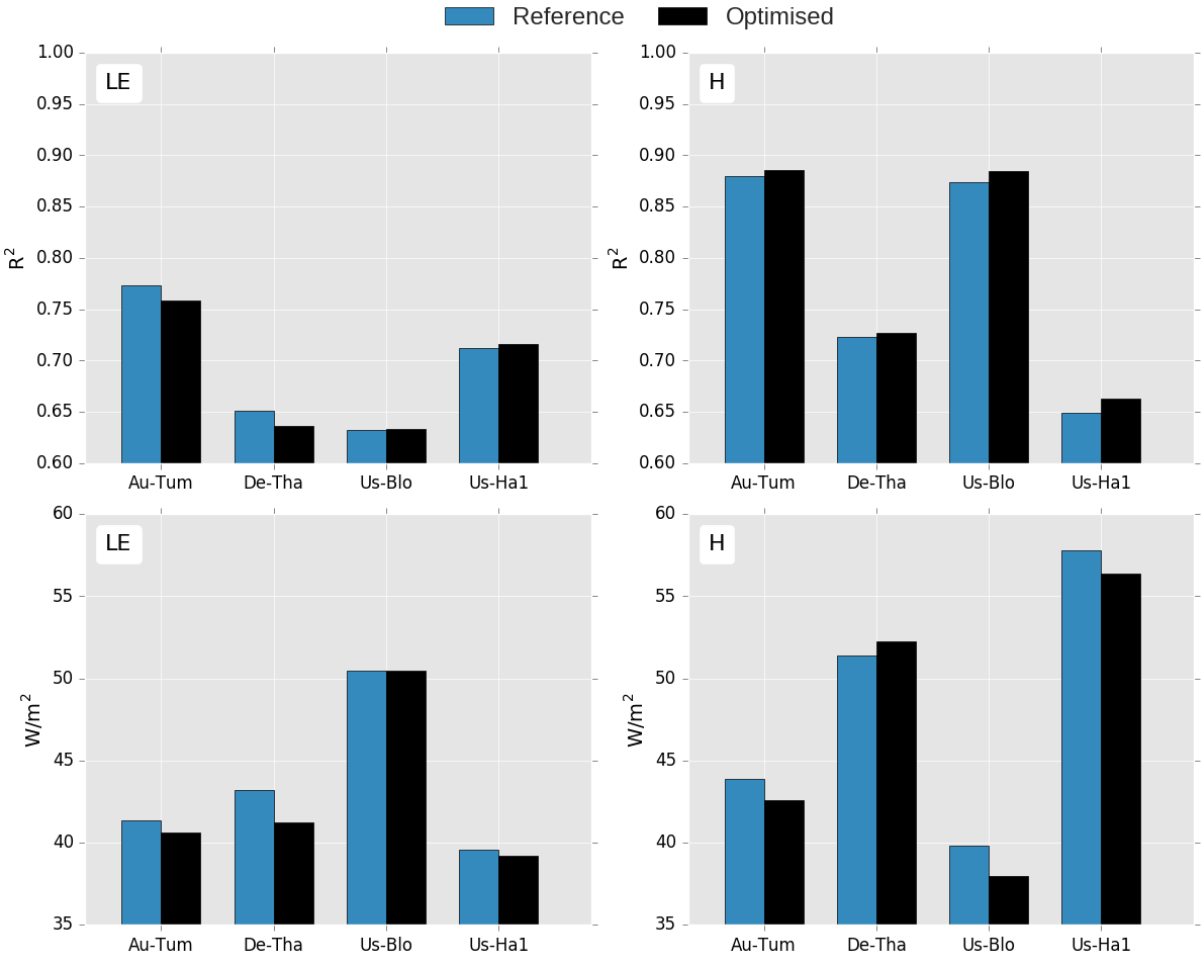

Figure 11. *Performance of simulated turbulent latent (LE) and sensible (H) heat fluxes with default (blue bars) and optimized (black bars) parameter prescriptions at the four forest study areas; Tumbarumba (Au-Tum), Tharandt (De-Tha), Blodgett (Us-Blo) and Harvard (Us-Ha1).The top row depict model fit (R2) and the bottom row average variance bias in Watt/m^2.*

6 Discussion

To contribute to the development of the SURFEX modeling platform this study set out to explore how sensitive ISBA-MEB simulated latent and sensible turbulent heat fluxes are to a selected set of uncertain parameters, to explore if parameter sensitivity patterns vary between forest environments and to evaluate how much model output improvement can be achieved by identifying site specific optimal prescription for the top most sensitive parameters. To achieve this, four forest areas with seasonal snow coverage representing different climate classifications and vegetation types was applied as model environments and the results of simulating these environments compared.

Parameter uncertainty was explored by Sobol sensitivity analysis. Sensitivity studies are commonly applied in ISBA related studies to evaluate impact of parameters as well as other input factors on modelled outputs. However, during the course of this study no prior ISBA related attempts to evaluate parameter impact on turbulent fluxes by applying the Sobol approach was identified. The influence of seven parameters on modelled turbulent latent and sensible heat was explored. In general, the parameter defining the ration between roughness length of momentum and thermal roughness length (ZOm/ZOh) was identified to be the top most sensitive for both latent and sensible heat fluxes. The second most sensitive parameter was identified to be the heat capacity of vegetation and soil (XUNIF_CV) and mainly influences simulations of sensible heat. Carrer et.al (2013) concluded that forest carbon fluxes are sensitive to ISBA parameters representing clumping index and leaf orientation at the top of the canopy, but less sensitive to parameters defining these aspects at canopy bottom. In contrast to the finding of Carrer et al. (2013), for turbulent fluxes of heat, only the leaf orientation parameter at canopy bottom (XXB_INF) is estimated to be highly influential primarily for latent heat. Remaining clumping index and leaf orientation parameters was seemingly non-influential in the context of the tested parameters. The same applies for the Longwave radiation transmission factor parameter (XTAU_LW).

For all sites except for Harvard forest the sensitivity analysis results are homogeneous. Harvard forest is the only site in which ZOm/ZOh did not have the highest sensitivity indices for H but instead exhibited neglectable sensitivity. In addition, in contrast to XXB_INF being non-sensitive at all sites for sensible heat this parameter was identified as the most influential for this flux variable at Harvard forest. This might be due to the fact that Harvard forest is the only site in which LAI has an annual cycle and parameters defining leaf characteristics may have greater influence on such sites. The fact that all four study areas were sensitive to the top two ranked parameters indicates that these results expand to multiple vegetation types and climatic characteristic. The fractional sensitivity of the total sensitivity of these parameters does however vary between study areas indicating that the influence of these parameters is site-specific.

Calibrating the highly sensitive parameters enabled simulations with lower cumulative latent and sensible variance with respect to observed time series for all sites than simulations with default parameter prescriptions. In general, the parameter values of the optimal vectors vary between sites. However, there is great bias in simulated LE and H with under and overestimations in terms of variance and model fit and it is therefore not possible to attribute

these variations to differences in environmental characteristics. In addition, the optimal values of the calibrated parameter vectors lie at the edges of the defined parameter ranges indicate that even greater variance reduction could be achieved by expanding parameter ranges. Such expansion would however generate unrealistic parameter prescriptions as such values would not be in accordance with the physical meaning of the parameters. This phenomena is interpreted as these values was selected, not due to the fact that they best represent the natural aspect represented by the parameters, but rather that these values best compensate for the great bias in the simulations. For Blodgett and Harvard forest some of the bias can be explained by simulated underestimates of Rn that consequently affects energy quantity available for partitioning. Napoly et al. (2016) describes that ISBA simulations of Gflux are lacking with great levels of under and overestimations which is the fact as well in the present study. However, as the factional proportion of Rn partitioned into Gflux is relatively small in comparison to LE and H this bias is not enough to explain but a fraction of the bias in the simulations. To explore the possibility of the bias being due to misrepresentative vegetation physiography parameters additional sensitivity studies were conducted. False prescriptions of physiography parameter applied to define the physical characteristics of the landscape were identified as the probable cause for bias Rn partitioning at De-Tha and Us-Blo as this bias was reduced by altering root depth and leaf area. Root depth governs how much soil water can be assimilated by vegetation and leaf area governs how much water can be used as a medium for latent heat emission. At the two American forests simulated Rn is underestimated which may be due to false prescription of albedo causing to high reflectance of incoming radiation or physiography parameters inhibiting radiation to reach the forest floor by penetrating the canopy. Identifying accurate physiography parameters is often problematic according to Muleta and Nicklow (2005) and it is highly unlikely to find accurate data for all inputs needed for a simulation. Hou et al. (2015) argues that is particularly problematic ins studies such as this one where inputs is derived from databases as these data is always to some degree generalised. Liu et al. (2004) describe that calibrating parameters in accordance with environmental prescriptions that are not representable for the target environment may lead to decreased variance between simulation and observations, but as the description of the landscape is inaccurate the calibrated parameters are not representable for the target environment. As neither the source of bias nor accurate parameter data could be derived no further emphasis was put on these aspects.

Nevertheless, by applying the cost function, parameter vectors are generated that reduce simulated cumulative LE and H variance at all four sites. However, as the cost function is not designed to consider individual variable variance reduction this do not necessarily mean that the variance for both output variables is decreased. Consequently, there were instances when the optimized vectors results in increased variance for one of the validation variables. The rate of variance reduction is directly related to the potential influence parameters have on validation variables. As such, even though the calibrated parameters were identified to hold the greatest proportional model influence in the context of all analysed parameters, optimizing these parameters given the applied methodology generate marginal variance reduction. Optimized vectors do in general generate better correspondence between simulated and

observed time series. However, as the cost function is not designed to evaluate model fit such improvement is not ensured.

Raoult et al. (2016) argues that sensitivity analysis and parameter calibration results are shaped by the modeller's subjective decisions such as what parameters to analyse and what values to test on these parameters. Even though the methodological applied in this study was designed to be as objective as possible it do included subjective elements. For instance, manually selecting a set of parameter candidates to include in the analysis is highly dependent on the knowledge of the model and the role of the parameters. An alternative approach applied by Liu et al. (2004) is to first conduct a preliminary screening of multiple parameters by the means of local sensitivity analysis to identify relevant parameter candidates. Local sensitivity analyses are less computational demanding than global approaches and can thus be applied to analyse a higher number of parameters for the same cost. Parameters identified as sensitive are then qualified for a more in in depth global analysis. Another benefit of this approach would be potential disclosure of parameter candidates that would otherwise not be considered as potentially sensitive.

Identifying an appropriate number of simulation iterations of the Sobol sensitivity analysis is crucial in deriving valid sensitivity indices. As there is no general consensus on how many iterations to perform this process becomes iterative and subjective as it depends on the complexity of the model and parameter interactions (Zhang et al., 2013). However, as a parameters first order index is a measure of the fractional sensitivity exhibited by that parameter all first order indices should add up to 1 and as total order indices measures first order indices plus all higher order indices due to interactions with remaining analysed parameters these indices should be 1 or more (Saltelli, 2008). Meticulous review of the sensitivity analysis results of the present study reveal that these requirements are not fulfilled at all sites as the total of all first order sensitivity indices do not sum to 1 and the total order indices are for some sites lower than 1 (Figure 5). This is due to computation errors that could be reduced by increasing the number of iterations. Tests were made to evaluate the impact on parameter indices by increasing simulation iterations which showed marginal changes to individual indices but the overall trend of sensitivity indications was however not altered.

Only data with energy closure imbalance (discussed in section 3.3) lower than 10 % was included in this study. This levels of energy imbalance is considered to be low and the fact that Napoly et.al (2016) noted in previous ISBA-MEB studies that closing the energy balance had neglectable impact on the simulations this issue was not further addressed. However, for even better calibration results the energy balance can been closed.

The choice of objective functions and design of cost functions used to evaluate parameter vectors performance in the calibration iterations greatly influence what parameter values are ranked as optimal. The cost function applied in this study was designed to considered variance bias but could be extended to also evaluate how well simulated time series correlate with dynamic diurnal and seasonal changes. As this cost function evaluate cumulative LE and H variance it is not ensured that optimized vectors decrease the bias of both flux variables if the variance reduction of one variable compensate for increased variance in the other. To further

develop the cost function considerations to this aspect such as these can be implemented. Finally, as the evaluated flux variables are measured in the same unit and the quantities of these fluxes are proportional, normalizing the flux variables in the cost function was redundant but did not affect the results of the study.

In light of the findings of the present study it is recommended that corrects prescriptions of parameters identified as highly sensitive is derived and applied in future simulations to decrease the uncertainty in modelled turbulent fluxes in forest regions. Furthermore, future parameter calibrations attempts should first include extended validation of physiography data applied to prescribe parameter if this data is derived from generalized data bases to ensure that the data is representable. This is important to enable high quality simulations catching the dynamic changes of fluxes and to ensure that optimized parameter vectors are calibrated in accordance with the intended environment. As optimized parameters are shaped by the objective function or cost function applied to evaluate parameter vector performance in the calibration process, careful considerations of what results are sought after prior to selecting or designing such performance metrics.

7 Conclusions

Sensitivity analysis disclosed that the uncertainty contribution of individual parameters to ISBA-MEB modelled turbulent latent and sensible heat fluxes varies between forest environments. However, out of the analysed parameters, modelled outputs were identified to be particularly sensitive to three parameters. The highest level of sensitivity is associated with the parameter representing the roughness length of momentum and thermal roughness length. In general, this parameter is associated with the highest level of sensitivity for both analysed model output variables. The second most sensitive is the parameter representing the heat capacity of vegetation and soil. It is primarily sensible heat that is sensitive to this parameter and for this variable it is the second most sensitive at all analysed study areas. A third parameter, representing the leaf orientation at canopy bottom, was identified to be significantly sensitive at three out of the four study areas. However, there is no general pattern neither in how sensitive the modelled flux variables are to this parameter nor which variable is sensitive to it. Instead, this parameter is ranked as the most, the second most and the third most sensitive for one or the other of the flux variables at different sites. Analysis of how the optimal numerical prescriptions of these highly sensitive parameters vary between forest environments was non-disclosing due to flaws in simulated flux time series supposedly resulting from bias in the physiography parameterisation. Nonetheless, results showed that calibrating the three top most sensitive parameters, by means of the applied methodology, reduce cumulative latent and sensible variance between simulated and validation flux time series at all four forest sites. In addition, this approach in general reduces the average variance of the individual flux variables by 0-2 W/m^2. However, at one site sensible heat variance was instead increased by applying calibrated parameters.

As it could not be derived from the results of this study, future research could further study if, and if so how, optimal parameter prescriptions vary between forest environments. In addition, evaluating if parameter sensitivity varies with seasonal phenology and weather cycles could be conducted for increased understanding of parameter model influence of such aspects. Furthermore, evaluating if parameter sensitivity patterns identified in this study can be extrapolated to similar forest areas can be conducted by multisite sensitivity study e.g. including several similar forest areas and exploring potential similarities and variations in parameter sensitivity. Finally, developing an automated parameter sensitivity and/or parameter calibration approach specifically for ISBA and/or ISBA-MEB could further aid in the development of the SURFEX modeling platform. In case of such endeavour, the methodology and developed algorithms of the present study could be considered.

References

Baldocchi, D, Falge, E, Lianhong, G, Olson, R, Hollinger, D, Running, S, Anthoni, P, Bernhofer, C et.al. 2001. FLUXNET: A New Tool to Study the Temporal and Spatial Variability of Ecosystem-Scale Carbon Dioxide, Water Vapor, and Energy Flux Densities. *Bulletin of the American Meteorological Society* 82: 2415-2434.

Barry, R, and Chorley, R. 2010. *Atmosphere, Weather and Climate*. London: Routledge.

Blyth, E, Gash, J, Lloyd, A, Pryor, M, Weedon, G, and Shuttleworth, J. 2010. Evaluating the JULES Land Surface Model Energy Fluxes Using FLUXNET Data. *Journal of Hydrometeorology* 11: 509-519.

Boone, A, Samuelsson, P, Gollvik, S, Napoly, A, Jarlan, L, Brun, E, and Decharme, B. 2017. The interactions between soil-biosphere-atmosphere land surface model with a multi-energy balance (ISBA-MEB) option in SURFEXv8 - Part 1: Model description. *Geoscientific Model Development* 10: 843-872.

Burba, G, & Anderson, D. 2010. *A Brief Practical Guide to Eddy Covariance Flux Measurements: Principles and Workflow Examples for Scientific and Industrial Applications.* Germany, Europe: LI-COR Biosciences

Carrer, D, Roujean, J, Lafont, S, Calvet, J, Boone, A, Decharme, B, Delire, C, and Gastellu-Etchegorry, J. 2013. A canopy radiative transfer scheme with explicit FAPAR for the interactive vegetation model ISBA-A-gs: Impact on carbon fluxes. *Journal of Geophysical Research-Biogeosciences* 118: 888-903.

Chaney, N, Herman, J, Ek, M, and Wood, E. 2016. Deriving global parameter estimates for the Noah land surface model using FLUXNET and machine learning. *Journal of Geophysical Research: Atmospheres* 121: 218-235.

Decharme, B, Boone, A, Delire, C, and Noilhan, J. 2011. Local evaluation of the Interaction between Soil Biosphere Atmosphere soil multilayer diffusion scheme using four pedotransfer functions. *Journal of Geophysical Research-Atmospheres* 116: 1-29.

Decharme, B, Martin, E, and Faroux, S. 2013. Reconciling soil thermal and hydrological lower boundary conditions in land surface models. *Journal of Geophysical Research: Atmospheres* 118: 7819-7834.

Decharme, B, Brun, E, Boone, A, Delire, C, Moigne, P. L, and Morin, S. 2016. Impacts of snow and organic soils parameterization on northern Eurasian soil temperature profiles simulated by the ISBA land surface model. *The Cryosphere* 10: 853-877.

Emery, C, Biancamaria, S, Boone, A, Garambois, P, Ricci, S, Rochoux, M, & Decharme, B. 2016. Temporal variance-based sensitivity analysis of the river-routing component of the large-scale hydrological model ISBA-TRIP: Application on the Amazon Basi. *Journal Of Hydrometeorology* 17: 3007-3027.

European flux database. 2017. Site detail.
Retrived 1 June, 2017, from http://gaia.agraria.unitus.it/home/site-details?id=8

Fares, S, McKay, M, Holzinger, R, & Goldstein, A .2010. Ozone fluxes in a Pinus ponderosa ecosystem are dominated by non-stomatal processes: Evidence from long-term continuous measurements. *Agricultural And Forest Meteorology* 150: 420-431.

FAO. 2017. Harmonized World Soil Database v 1.2.
Retrieved 1 June, 2017, from http://www.fao.org/soils-portal/soil-survey/soil-maps-and-databases/harmonized-world-soil-database-v12/en/

Freedman, J, Fitzjarrald, D, Moore, K, & Sakai, R .2001. Boundary layer clouds and vegetation-atmosphere feedbacks. *Journal Of Climate*, 14: 180-197.

Goldstein, A, Goulden, M, Munger, J, Wofsy, S, & Geron, C. 1998. Seasonal course of isoprene emissions from a midlatitude deciduous forest. *Journal Of Geophysical Research. Atmospheres* 103: 31045.

Goldstein, A, Hultman, N, Fracheboud, J, Bauer, M, Panek, J, Xu, M, Qi, Y, Guenther, A, & Baugh, W. 2000. Effects of climate variability on the carbon dioxide, water, and sensible heat fluxes above a ponderosa pine plantation in the Sierra Nevada (CA). *Agricultural And Forest Meteorology* 101: 113-129.

Grüwald, T, & Bernhofer, C. 2007. A decade of carbon, water and energy flux measurements of an old spruce forest at the Anchor Station Tharandt. *Tellus: Series B* 59: 387-396.

Herman, J. and Usher, W. 2017. SALib: An open-source Python library for sensitivity analysis. *Journal of Open Source Software* 2.

Hou, T, Zhu, Y, Lü, H, Yu, Z, Ouyang, F, & Sudicky, E. 2015. Parameter sensitivity analysis and optimization of Noah land surface model with field measurements from Huaihe River Basin, China. *Stochastic Environmental Research And Risk Assessment* 29: 1383-1401.

Joetzjer, E, Delire, C, Douville, H, Ciais, P, Decharme, B, Carrer, D, Verbeeck, H, De Weirdt, M, & Bonal, D. 2015. Improving the ISBACC land surface model simulation of water and carbon fluxes and stocks over the Amazon forest. *Geoscientific Model Development* 8: 1709-1727.

Karan, M, Liddell, M, Prober, S, Arndt, S, Beringer, J, Boer, M, Cleverly, J, Eamus, D et.al. 2016. The Australian SuperSite Network: A continental, long-term terrestrial ecosystem observatory. *Science Of The Total Environment* 568: 1263-1274.

Keith, H, Leuning, R, Jacobsen, K, Cleugh, H, van Gorsel, E, Raison, R, Medlyn, B, Winters, A, & Keitel, C. 2009. Multiple measurements constrain estimates of net carbon exchange by a Eucalyptus forest. *Agricultural And Forest Meteorology* 149: 535-558

Leuning, R, Cleugh, H, Zegelin, S, & Hughes, D. 2005. Carbon and water fluxes over a temperate Eucalyptus forest and a tropical wet/dry savanna in Australia: measurements and comparison with MODIS remote sensing estimates. *Agricultural And Forest Meteorology* 129: 151-173.

Liming, H, Chen, J, Pisek, J, Schaaf, C, & Strahler, A. 2012. Global clumping index map derived from the MODIS BRDF product. *Remote Sensing Of Environment* 119: 118-130.

Liu, Y, Gupta, H, Sorooshian, S, Bastidas, L, & Shuttleworth, W. 2004. Exploring parameter sensitivities of the land surface using a locally coupled land-atmosphere model. *Journal Of Geophysical Research. Atmospheres*: 109: D21101.

Majozi, N, Mannaerts, C, Ramoelo, A, Mathieu, R, Nickless, A, & Verhoef, W. 2017. Analysing surface energy balance closure and partitioning over a semi-arid savanna FLUXNET site in Skukuza, Kruger National Park, South Africa. *Hydrology & Earth System Sciences Discussions* 21: 3401-3415.

Masson, V., Moigne, P. L., Martin, E., Faroux, S., Alias, A., Alkama, R., Belamari, S., Barbu et.al 2013. The SURFEXv7.2 land and ocean surface platform for coupled or offline

simulation of earth surface variables and fluxes. *Geoscientific Model Development* 6: 929-960.

Muleta, M, & Nicklow, J. 2005. Sensitivity and uncertainty analysis coupled with automatic calibration for a distributed watershed model. *Journal Of Hydrology* 306: 127-145.

Napoly, A, Boone, A, Samuelsson, P, Gollvik, S, Martin, E, Seferian, R, Carrer, D, Decharme, B, & Jarlan, L. 2016. The Interactions between Soil-Biosphere-Atmosphere (ISBA) land surface model Multi-Energy Balance (MEB) option in SURFEX - Part 2: Model evaluation for local scale forest sites', *Geoscientific Model Development Discussions*. 1-40

Overgaard, J, Rosbjerg, D and Butts, M. B. 2006. Land-surface modeling in hydrological perspective – a review', *Biogeosciences* 3: 229-241.

Pelletier, J, Field J. 2016. Predicting the roughness length of turbulent flows over landscapes with multi-scale microtopography. *Earth Surface Dynamics* 4: 391-405.

Pianosi, F, Iwema, J, Rosolem, R, & Wagener, T. 2017. Chapter 7: A Multimethod Global Sensitivity Analysis Approach to Support the Calibration and Evaluation of Land Surface Models. *Sensitivity Analysis In Earth Observation Modelling:* 125-144.

Raoult, N. M., Jupp, T. E., Cox, P. M., and Luke, C. M. 2016. Land-surface parameter optimisation using data assimilation techniques: the adJULES system V1.0, *Geosci. Model Dev.* 9: 2833-2852.

Richardson, A, Hollinger, D, Burba, G, Davis, K, Flanagan, L, Katul, G, William Munger, J, Ricciuto, D et.al. 2006. A multi-site analysis of random error in tower-based measurements of carbon and energy fluxes. *Agricultural And Forest Meteorology* 136: 1-18.

Rosero, E, Yang, Z, Wagener, T, Gulden, L, Yatheendradas, S, & Niu, G n.d. 2010. Quantifying parameter sensitivity, interaction, and transferability in hydrologically enhanced versions of the Noah land surface model over transition zones during the warm season. *Journal Of Geophysical Research-Atmospheres* 115: D03106.

Saltelli, A. 2008. *Global sensitivity analysis: the primer*. Chichester, England; Hoboken, NJ: John Wiley.

Sauer , T & Horton, R. 2005. Soil Heat Flux. *Micrometeorology in Agricultural Systems, Agronomy Monograph* 47: 131-154.

Savoy, P, & Mackay, D. 2015. Modeling the seasonal dynamics of leaf area index based on environmental constraints to canopy development. *Agricultural And Forest Meteorology* 200: 46-56.

Schwärzel, K, Menzer, A, Clausnitzer, F, Spank, U, Häntzschel, J, Grünwald, T, Köstner, B, Bernhofer, C et.al. 2009. Soil water content measurements deliver reliable estimates of water fluxes: A comparative study in a beech and a spruce stand in the Tharandt forest (Saxony, Germany). *Agricultural & Forest Meteorology* 149: 1994-2006.

Sobol' IM. 1993. Sensitivity estimates for nonlinear mathematical models. *Math Model Comput* Exp 1: 407–417.

Tang Y, Reed P, Wagener T, Van Werkhoven K. 2007. Comparing sensitivity analysis methods to advance lumped watershed model identification and evaluation. *Hydrology And Earth System Sciences* 11: 793-817.

Urbanski, S, Barford, C, Wofsy, S, Kucharik, C, Pyle, E, Budney, J, McKain, K, Fitzjarrald, D et.al. 2007. Factors controlling CO2 exchange on timescales from hourly to decadal at Harvard Forest. *Journal Of Geophysical Research-Biogeosciences* 112: G2.

Van Der Walt, S, Colbert, S, & Varoquaux, G. 2011. The NumPy Array: A Structure for Efficient Numerical Computation. *Computing In Science & Engineering, Comput. Sci* 2: 22-30.

Wild, M, Folini, D, Hakuba, M, Schär, C, Seneviratne, S, Kato, S, Rutan, D, Ammann, C et.al. 2015. The energy balance over land and oceans: an assessment based on direct observations and CMIP5 climate models. *Climate Dynamics* 44: 3393-3429.

Zhang, C, Chu, J, & Fu, G .2013. Sobol's sensitivity analysis for a distributed hydrological model of Yichun River Basin, China. *Journal Of Hydrology* 480: 58-68.

Zhao, W, & Li, A. 2015. A Review on Land Surface Processes Modeling over Complex Terrain. *Advances In Meteorology* 2015: 1-17.

Series from Lund University

Department of Physical Geography and Ecosystem Science

Master Thesis in Geographical Information Science

1. *Anthony Lawther:* The application of GIS-based binary logistic regression for slope failure susceptibility mapping in the Western Grampian Mountains, Scotland (2008).
2. *Rickard Hansen:* Daily mobility in Grenoble Metropolitan Region, France. Applied GIS methods in time geographical research (2008).
3. *Emil Bayramov:* Environmental monitoring of bio-restoration activities using GIS and Remote Sensing (2009).
4. *Rafael Villarreal Pacheco:* Applications of Geographic Information Systems as an analytical and visualization tool for mass real estate valuation: a case study of Fontibon District, Bogota, Columbia (2009).
5. *Siri Oestreich Waage:* a case study of route solving for oversized transport: The use of GIS functionalities in transport of transformers, as part of maintaining a reliable power infrastructure (2010).
6. *Edgar Pimiento:* Shallow landslide susceptibility – Modelling and validation (2010).
7. *Martina Schäfer:* Near real-time mapping of floodwater mosquito breeding sites using aerial photographs (2010).
8. *August Pieter van Waarden-Nagel:* Land use evaluation to assess the outcome of the programme of rehabilitation measures for the river Rhine in the Netherlands (2010).
9. *Samira Muhammad:* Development and implementation of air quality data mart for Ontario, Canada: A case study of air quality in Ontario using OLAP tool. (2010).
10. *Fredros Oketch Okumu*: Using remotely sensed data to explore spatial and temporal relationships between photosynthetic productivity of vegetation and malaria transmission intensities in selected parts of Africa (2011).
11. *Svajunas Plunge:* Advanced decision support methods for solving diffuse water pollution problems (2011).
12. *Jonathan Higgins:* Monitoring urban growth in greater Lagos: A case study using GIS to monitor the urban growth of Lagos 1990 - 2008 and produce future growth prospects for the city (2011).
13. *Mårten Karlberg:* Mobile Map Client API: Design and Implementation for Android (2011).
14. *Jeanette McBride:* Mapping Chicago area urban tree canopy using color infrared imagery (2011).
15. *Andrew Farina:* Exploring the relationship between land surface temperature and vegetation abundance for urban heat island mitigation in Seville, Spain (2011).

16. *David Kanyari*: Nairobi City Journey Planner: An online and a Mobile Application (2011).
17. *Laura V. Drews:* Multi-criteria GIS analysis for siting of small wind power plants - A case study from Berlin (2012).
18. *Qaisar Nadeem:* Best living neighborhood in the city - A GIS based multi criteria evaluation of ArRiyadh City (2012).
19. *Ahmed Mohamed El Saeid Mustafa:* Development of a photo voltaic building rooftop integration analysis tool for GIS for Dokki District, Cairo, Egypt (2012).
20. *Daniel Patrick Taylor*: Eastern Oyster Aquaculture: Estuarine Remediation via Site Suitability and Spatially Explicit Carrying Capacity Modeling in Virginia's Chesapeake Bay (2013).
21. *Angeleta Oveta Wilson:* A Participatory GIS approach to *unearthing* Manchester's Cultural Heritage '*gold mine'* (2013).
22. *Ola Svensson:* Visibility and Tholos Tombs in the Messenian Landscape: A Comparative Case Study of the Pylian Hinterlands and the Soulima Valley (2013).
23. *Monika Ogden:* Land use impact on water quality in two river systems in South Africa (2013).
24. *Stefan Rova:* A GIS based approach assessing phosphorus load impact on Lake Flaten in Salem, Sweden (2013).
25. *Yann Buhot:* Analysis of the history of landscape changes over a period of 200 years. How can we predict past landscape pattern scenario and the impact on habitat diversity? (2013).
26. *Christina Fotiou:* Evaluating habitat suitability and spectral heterogeneity models to predict weed species presence (2014).
27. *Inese Linuza:* Accuracy Assessment in Glacier Change Analysis (2014).
28. *Agnieszka Griffin:* Domestic energy consumption and social living standards: a GIS analysis within the Greater London Authority area (2014).
29. *Brynja Guðmundsdóttir:* Detection of potential arable land with remote sensing and GIS - A Case Study for Kjósarhreppur (2014).
30. *Oleksandr Nekrasov:* Processing of MODIS Vegetation Indices for analysis of agricultural droughts in the southern Ukraine between the years 2000-2012 (2014).
31. *Sarah Tressel:* Recommendations for a polar Earth science portal in the context of Arctic Spatial Data Infrastructure (2014).
32. *Caroline Gevaert:* Combining Hyperspectral UAV and Multispectral Formosat-2 Imagery for Precision Agriculture Applications (2014).
33. *Salem Jamal-Uddeen:* Using GeoTools to implement the multi-criteria evaluation analysis - weighted linear combination model (2014).
34. *Samanah Seyedi-Shandiz:* Schematic representation of geographical railway network at the Swedish Transport Administration (2014).
35. *Kazi Masel Ullah:* Urban Land-use planning using Geographical Information System and analytical hierarchy process: case study Dhaka City (2014).

36. *Alexia Chang-Wailing Spitteler:* Development of a web application based on MCDA and GIS for the decision support of river and floodplain rehabilitation projects (2014).
37. *Alessandro De Martino:* Geographic accessibility analysis and evaluation of potential changes to the public transportation system in the City of Milan (2014).
38. *Alireza Mollasalehi:* GIS Based Modelling for Fuel Reduction Using Controlled Burn in Australia. Case Study: Logan City, QLD (2015).
39. *Negin A. Sanati:* Chronic Kidney Disease Mortality in Costa Rica; Geographical Distribution, Spatial Analysis and Non-traditional Risk Factors (2015).
40. *Karen McIntyre:* Benthic mapping of the Bluefields Bay fish sanctuary, Jamaica (2015).
41. *Kees van Duijvendijk:* Feasibility of a low-cost weather sensor network for agricultural purposes: A preliminary assessment (2015).
42. *Sebastian Andersson Hylander:* Evaluation of cultural ecosystem services using GIS (2015).
43. *Deborah Bowyer:* Measuring Urban Growth, Urban Form and Accessibility as Indicators of Urban Sprawl in Hamilton, New Zealand (2015).
44. *Stefan Arvidsson:* Relationship between tree species composition and phenology extracted from satellite data in Swedish forests (2015).
45. *Damián Giménez Cruz*: GIS-based optimal localisation of beekeeping in rural Kenya (2016).
46. *Alejandra Narváez Vallejo:* Can the introduction of the topographic indices in LPJ-GUESS improve the spatial representation of environmental variables? (2016).
47. *Anna Lundgren:* Development of a method for mapping the highest coastline in Sweden using breaklines extracted from high resolution digital elevation models (2016).
48. *Oluwatomi Esther Adejoro:* Does location also matter? A spatial analysis of social achievements of young South Australians (2016).
49. *Hristo Dobrev Tomov:* Automated temporal NDVI analysis over the Middle East for the period 1982 - 2010 (2016).
50. *Vincent Muller:* Impact of Security Context on Mobile Clinic Activities A GIS Multi Criteria Evaluation based on an MSF Humanitarian Mission in Cameroon (2016).
51. *Gezahagn Negash Seboka:* Spatial Assessment of NDVI as an Indicator of Desertification in Ethiopia using Remote Sensing and GIS (2016).
52. *Holly Buhler:* Evaluation of Interfacility Medical Transport Journey Times in Southeastern British Columbia. (2016).
53. *Lars Ole Grottenberg*: Assessing the ability to share spatial data between emergency management organisations in the High North (2016).
54. *Sean Grant:* The Right Tree in the Right Place: Using GIS to Maximize the Net Benefits from Urban Forests (2016).

55. *Irshad Jamal:* Multi-Criteria GIS Analysis for School Site Selection in Gorno-Badakhshan Autonomous Oblast, Tajikistan (2016).
56. *Fulgencio Sanmartín:* Wisdom-volkano: A novel tool based on open GIS and time-series visualization to analyse and share volcanic data (2016).
57. *Nezha Acil:* Remote sensing-based monitoring of snow cover dynamics and its influence on vegetation growth in the Middle Atlas Mountains (2016).
58. *Julia Hjalmarsson:* A Weighty Issue: Estimation of Fire Size with Geographically Weighted Logistic Regression (2016).
59. *Mathewos Tamiru Amato:* Using multi-criteria evaluation and GIS for chronic food and nutrition insecurity indicators analysis in Ethiopia (2016).
60. *Karim Alaa El Din Mohamed Soliman El Attar:* Bicycling Suitability in Downtown, Cairo, Egypt (2016).
61. *Gilbert Akol Echelai:* Asset Management: Integrating GIS as a Decision Support Tool in Meter Management in National Water and Sewerage Corporation (2016).
62. *Terje Slinning:* Analytic comparison of multibeam echo soundings (2016).
63. *Gréta Hlín Sveinsdóttir:* GIS-based MCDA for decision support: A framework for wind farm siting in Iceland (2017).
64. *Jonas Sjögren:* Consequences of a flood in Kristianstad, Sweden: A GIS-based analysis of impacts on important societal functions (2017).
65. *Nadine Raska:* 3D geologic subsurface modelling within the Mackenzie Plain, Northwest Territories, Canada (2017).
66. *Panagiotis Symeonidis*: Study of spatial and temporal variation of atmospheric optical parameters and their relation with PM 2.5 concentration over Europe using GIS technologies (2017).
67. *Michaela Bobeck:* A GIS-based Multi-Criteria Decision Analysis of Wind Farm Site Suitability in New South Wales, Australia, from a Sustainable Development Perspective (2017).
68. *Raghdaa Eissa*: Developing a GIS Model for the Assessment of Outdoor Recreational Facilities in New Cities Case Study: Tenth of Ramadan City, Egypt (2017).
69. *Zahra Khais Shahid*: Biofuel plantations and isoprene emissions in Svea and Götaland (2017).
70. *Mirza Amir Liaquat Baig*: Using geographical information systems in epidemiology: Mapping and analyzing occurrence of diarrhea in urban - residential area of Islamabad, Pakistan (2017).
71. *Joakim Jörwall*: Quantitative model of Present and Future well-being in the EU-28: A spatial Multi-Criteria Evaluation of socioeconomic and climatic comfort factors (2017).
72. *Elin Haettner*: Energy Poverty in the Dublin Region: Modelling Geographies of Risk (2017).
73. *Harry Eriksson*: Geochemistry of stream plants and its statistical relations to soil- and bedrock geology, slope directions and till geochemistry. A GIS-analysis of small catchments in northern Sweden. (2017).

74. *Daniel Gardevärn:* PPGIS and Public meetings – An evaluation of public participation methods for urban planning. (2017).
75. *Kim Friberg:* Sensitivity Analysis and Calibration of Multi Energy Balance Land Surface Model Parameters. (2017).